

INTEGRATED *UBV* PHOTOMETRY OF 624 STAR CLUSTERS AND ASSOCIATIONS IN THE LARGE MAGELLANIC CLOUD

E. BICA^{1,2}

Instituto de Física, Universidade Federal do Rio Grande do Sul, Avenida Bento Gonçalves 9500, C.P. 15051, CEP 91501-970, Porto Alegre, RS, Brazil;
 bica@if1.if.ufrgs.br

J. J. CLARIÁ²

Observatorio Astronómico, Universidad Nacional de Córdoba, Laprida 854, 5000 Córdoba, Argentina; claria@uncbob.edu.ar

H. DOTTORI² AND J. F. C. SANTOS, JR.¹

Instituto de Física, Universidade Federal do Rio Grande do Sul, Avenida Bento Gonçalves 9500, C.P. 15051, CEP 91501-970, Porto Alegre, RS, Brazil;
 dottori, joao@if1.if.ufrgs.br

AND

A. E. PIATTI^{1,2}

Observatorio Astronómico, Universidad Nacional de Córdoba, Laprida 854, 5000 Córdoba, Argentina; piatti@uncbob.edu.ar

Received 1995 February 6; accepted 1995 June 29

ABSTRACT

We present a catalog of integrated *UBV* photometry of 504 star clusters and 120 stellar associations in the LMC, part of them still embedded in emitting gas. We study age groups in terms of equivalent SWB types derived from the $(U-B) \times (B-V)$ diagram. The size of the spatial distributions increases steadily with age (SWB types), whereas a difference of axial ratio exists between the groups younger than 30 Myr and those older, which implies a nearly face-on orientation for the former and a tilt of $\sim 45^\circ$ for the latter groups. Asymmetries are present in the spatial distributions, which, together with the noncoincidence of the centroids for different age groups, suggest that the LMC disk was severely perturbed in the past.

Subject headings: catalogs — galaxies: star clusters — galaxies: photometry — Magellanic Clouds

1. INTRODUCTION

Integrated photometry of star clusters provides fundamental insight on the star-formation history of the Large Magellanic Cloud (see van den Bergh 1991 for a review). A compilation of *UBV* photometry for ~ 140 LMC clusters was made by van den Bergh (1981, hereafter VDB81). However, the number of cataloged clusters in the LMC is ~ 2000 (see Hodge 1988 and references therein). The cluster sample that is suitable for aperture photometry is not as large, but a simple inspection of the LMC atlas (Hodge & Wright 1967) or the Sky Survey plates shows that about half of them can be observed easily with photoelectric photometry.

In the present work we provide a catalog of integrated *UBV* photometry of star clusters and associations in the LMC, which increases the sample by a factor of ~ 5 with respect to that in VDB81. Part of the present sample has been discussed in previous papers: Bica et al. (1991) called attention to a gap detected in the color-color diagram, and Bica, Clariá, & Dottori (1992, hereafter BCD92) analyzed the properties of the clusters

¹Visiting Astronomer, Cerro Tololo Inter-American Observatory, operated by AURA, Chile.

²Visiting Astronomer, Complejo Astronómico El Leoncito, operated under agreement between the Consejo Nacional de Investigaciones Científicas y Técnicas de la República Argentina and the National Universities of La Plata, Córdoba, and San Juan, Argentina.

in the bar region. The present large sample and the classification of the objects in age groups allow the study in detail of the evolution of the spatial properties with a suitable time resolution.

We present the observations and catalog in § 2. A discussion of the properties of the color-color diagram for star clusters and associations, as well as the derivation of equivalent SWB types (Searle, Wilkinson, & Bagnuolo 1980, hereafter SWB) is given in § 3. The spatial distribution of the age groups is analyzed in § 4. Concluding remarks are given in § 5.

2. OBSERVATIONS

We selected the sample objects on Hodge & Wright's (1967) LMC atlas and on the J and R plates of the ESO/SERC Southern Sky Survey atlases; we searched for the brighter star clusters and associations (including those related to emitting gas), also based on information in the existing catalogs. The *V* magnitude histograms (see § 3) provide hints on the sample's completeness. Column (1) of Table 1 lists the objects, with the following catalog designations: H (Hodge 1960), SL (Shapley & Lindsay 1963), LW (Lyngå & Westerlund 1963), HS (Hodge & Sexton 1966), ESO (Lauberts 1982), H88- (Hodge 1988), BRHT (Bhatia et al. 1991), KMK88- (Kontizas, Metaxa, & Kontizas 1988), KMHK (Kontizas et al. 1990), LH (Lucke & Hodge 1970), N (Henize 1956), DEM (Davies, Elliot, & Meab-

TABLE 1
CATALOG OF INTEGRATED *UBV* PHOTOMETRY

| NAME | D(°) | V | U-B | B-V | X(°) | Y(°) | SWB | TYPE |
|---|------|-------|-------|-------|------|-------|-----|------|
| NGC1466=SL1=LW1 | 60V | 11.59 | 0.13 | 0.68 | 7.53 | -2.30 | VII | C |
| NGC1629=SL3=LW3 | 38C | 14.08 | 0.30 | 0.95 | 3.96 | -2.42 | VI | C |
| RETICULUM=Sersic40/3=ESO118SC31=KMHK10 | 113C | 14.25 | 0.26 | 0.59 | 5.92 | 10.56 | VII | C |
| NGC1644=SL9=LW11 | 61V | 12.89 | 0.22 | 0.63 | 4.41 | 3.23 | V | C |
| NGC1651=SL7=LW12 | 100T | 12.28 | 0.28 | 0.71 | 3.59 | -1.16 | V | C |
| SL8=LW13 | 61C | 13.80 | 0.11 | 0.76 | 3.86 | 0.40 | VII | C |
| NGC1652=SL10=LW14 | 62VC | 13.13 | 0.28 | 0.82 | 3.88 | 0.76 | VI | C |
| SL11=LW16 | 61C | 13.80 | 0.30 | 0.76 | 3.38 | -1.57 | VI | C |
| SL14=LW21 | 40T | 13.88 | -0.25 | 0.20 | 3.51 | -0.22 | II | C |
| SL28=LW47 | 61C | 13.53 | 0.16 | 0.65 | 2.39 | -4.82 | V | C |
| NGC1673=SL17=LW31 | 19C | 14.07 | -0.12 | 0.45 | 3.29 | -0.39 | III | C |
| SL37=LW61 | 61C | 13.39 | 0.26 | 0.84 | 2.54 | -2.96 | VI | C |
| NGC1693=SL39 | 50T | 12.89 | -0.40 | 0.26 | 2.93 | 0.10 | I | C |
| NGC1695=SL40 | 50T | 12.16 | -0.12 | 0.34 | 2.92 | 0.06 | III | C |
| SL41=LW64 | 38C | 14.14 | 0.33 | 0.74 | 2.46 | -3.15 | V | C |
| NGC1696=SL43 | 38C | 13.95 | 0.02 | 0.49 | 3.02 | 1.20 | IVA | C |
| NGC1697=SL44 | 50T | 12.62 | 0.23 | 0.53 | 2.96 | 0.88 | IVB | C |
| NGC1698=SL45 | 40T | 12.07 | -0.31 | 0.17 | 2.84 | 0.33 | I | C |
| IC2105=N77A (in DEM 4b) | 34T | 12.78 | -0.89 | -0.10 | 2.80 | 0.24 | 0 | NC |
| NGC1702=SL46 | 50T | 12.50 | -0.26 | 0.18 | 2.70 | -0.41 | II | C |
| SL49 | 34T | 12.28 | -0.48 | 0.33 | 2.76 | 0.44 | I | C |
| NGC1704=SL50 | 72V | 11.50 | -0.40 | 0.28 | 2.68 | -0.32 | I | C |
| SL56 | 45V | 12.26 | -0.29 | 0.19 | 2.58 | -0.63 | II | C |
| NGC1711=SL55 | 60V | 10.11 | -0.37 | 0.12 | 2.59 | -0.54 | I | C |
| SL58 | 50T | 12.50 | -0.04 | 0.27 | 2.60 | -0.19 | III | C |
| NGC1712=SL60=LH1w (in N79) | 150T | 9.86 | -0.55 | 0.16 | 2.63 | 0.04 | I | AN |
| NGC1714=N4A=SL64=DEM8b | 50T | 11.61 | -0.69 | -0.10 | 2.86 | 2.52 | 0 | NC |
| SL61=LW79 | 61C | 13.99 | 0.27 | 0.59 | 1.80 | -6.09 | V | C |
| SL66 | 38C | 13.46 | 0.24 | 0.78 | 2.42 | -0.95 | VI | C |
| NGC1718=SL65 | 62V | 12.25 | 0.26 | 0.76 | 2.81 | 2.39 | VI | C |
| IC2111 (in N79A=BRHT1b,in NGC1722=LH1e,in DEM210) | 34T | 12.46 | -0.86 | -0.13 | 2.56 | 0.05 | 0 | NC |
| BRHT1a (in NGC1722=LH1e,in DEM210) | 50T | 13.22 | -0.54 | -0.05 | 2.55 | 0.04 | 0 | NC |
| NGC1727=N79E=SL67=LH2 (in DEM10) | 100T | 11.06 | -1.01 | -0.18 | 2.54 | 0.11 | 0 | NA |
| SL69 (in N5=DEM11,in LH3) | 100T | 12.06 | -0.97 | -0.22 | 2.77 | 2.19 | 0 | NA |
| SL75 | 50T | 12.72 | -0.06 | 0.21 | 2.53 | 0.53 | III | C |
| SL76 | 40T | 12.08 | 0.05 | 0.17 | 2.59 | 1.23 | III | C |
| NGC1731=N4D=LH4=DEM12 | 150T | 9.94 | -0.84 | -0.11 | 2.72 | 2.52 | 0 | NA |
| SL79=LW85 | 50T | 13.44 | 0.03 | 0.29 | 2.18 | -2.21 | III | C |
| NGC1732=SL77 | 45V | 12.30 | -0.20 | 0.14 | 2.53 | 0.79 | II | C |
| SL81 (in LH3) | 100T | 12.04 | -0.54 | 0.08 | 2.69 | 2.04 | I | A |
| NGC1733=SL85 | 50T | 13.31 | 0.10 | 0.35 | 2.69 | 2.76 | IVA | C |
| NGC1734=SL83 | 50T | 13.10 | 0.05 | 0.22 | 2.49 | 0.68 | III | C |
| NGC1735=SL86 | 72V | 10.76 | -0.28 | 0.12 | 2.62 | 2.35 | II | C |
| NGC1736=N8 (in DEM13) | 100T | 11.85 | -0.90 | -0.25 | 2.62 | 1.39 | 0 | NA |
| SL84=LW89 | 38C | 14.38 | 0.15 | 0.62 | 1.74 | -5.63 | IVB | C |
| NGC1737=DEM22a (in N83=LH5=DEM22) | 50T | 13.18 | -0.84 | 0.00 | 2.40 | 0.28 | 0 | NA |
| NGC1743=N83A=SL87 (in DEM22b,in N83=LH5) | 50T | 11.26 | -0.81 | -0.18 | 2.39 | 0.25 | 0 | NC |
| NGC1745 (in DEM22d,in N83=LH5=DEM22) | 50T | 13.40 | -1.02 | -0.16 | 2.38 | 0.28 | 0 | NA |
| NGC1748=IC2114=N83B (in N83=LH5=DEM22) | 50T | 12.24 | -0.92 | -0.15 | 2.36 | 0.26 | 0 | NC |
| NGC1747=LH6 (in N9) | 150T | 9.37 | -0.71 | 0.04 | 2.53 | 2.28 | I | AN |
| SL92 | 38C | 14.46 | 0.10 | 0.60 | 2.47 | 1.20 | IVB | C |
| NGC1751=SL89 | 100T | 11.73 | 0.27 | 0.79 | 2.30 | -0.36 | VI | C |
| NGC1754=SL91 | 100T | 11.57 | 0.15 | 0.75 | 2.21 | -0.99 | VII | C |
| NGC1749=SL93 | 50T | 13.56 | -0.34 | 0.03 | 2.43 | 1.26 | II | C |
| NGC1755=SL99 | 72V | 9.85 | -0.20 | 0.16 | 2.40 | 1.24 | II | C |
| NGC1756=SL94 | 72V | 12.24 | 0.09 | 0.40 | 2.32 | 0.21 | IVA | C |
| SL105 | 40T | 12.25 | -0.11 | 0.23 | 2.35 | 0.91 | III | C |
| SL106 | 72V | 11.28 | -0.33 | 0.15 | 2.24 | -0.23 | I | C |
| NGC1760=N11F (in LH9,in N11,in N10) | 100T | 11.46 | -0.97 | -0.09 | 2.45 | 2.92 | 0 | NA |
| BCDSP1 (in LH9,in N11,in N10) | 100T | 10.71 | -0.78 | 0.33 | 2.49 | 3.00 | I | A |
| NGC1761=SL122 (in LH9,in N11,in N10) | 150T | 9.94 | -0.90 | -0.07 | 2.47 | 2.97 | 0 | A |
| HD32228=KMHK307 (in NGC1761) | 40T | 10.64 | -0.91 | -0.17 | 2.48 | 2.98 | 0 | C |
| NGC1763w=N11Bw=SL125w=LH10w (in N11) | 150T | 9.40 | -0.84 | -0.11 | 2.47 | 3.04 | 0 | NA |
| NGC1763e=N11Be=SL125e=LH10e (in N11) | 150T | 9.64 | -0.89 | -0.14 | 2.43 | 3.04 | 0 | NA |
| IC2116=N11A (in N11=DEM34,in N10) | 40T | 12.66 | -0.80 | -0.19 | 2.41 | 3.08 | 0 | NC |
| LH7 (Includes SL111 and BRHT25b) | 100T | 11.93 | -0.18 | 0.29 | 2.00 | -1.93 | II | A |
| NGC1769=LH13=N11C (in N11,in N10) | 150T | 9.97 | -0.83 | -0.15 | 2.36 | 2.99 | 0 | NA |
| SL109 (in LH8=DEM36) | 50T | 12.49 | -0.83 | -0.11 | 2.22 | -0.05 | 0 | C |
| BRHT25b=KMHK312 (in LH7) | 40T | 13.70 | -0.35 | 0.04 | 1.97 | -1.97 | II | C |
| HNT1 (in NGC1769,in N11,in N10) | 40T | 12.44 | -0.63 | -0.01 | 2.37 | 2.97 | 0 | NC |
| NGC1764=SL115 | 40T | 12.58 | -0.35 | 0.34 | 2.35 | 1.75 | I | C |
| SL110 | 100T | 13.30 | -0.07 | 0.37 | 2.25 | 0.29 | III | C |
| SL114 | 50T | 11.46 | -0.75 | 0.00 | 2.20 | 0.20 | 0 | C |
| NGC1766=SL113 | 72V | 12.22 | -0.51 | 0.11 | 2.10 | -0.78 | I | C |
| SL116 | 50T | 12.25 | -0.18 | 0.20 | 2.22 | 0.64 | II | C |
| SL117 | 50T | 12.28 | -0.06 | 0.25 | 2.21 | 0.48 | III | C |
| SL119 | 100T | 12.44 | 0.11 | 0.64 | 2.28 | 1.28 | IVB | C |
| SL123 (in LH8=DEM36) | 100T | 11.81 | -0.71 | -0.08 | 2.15 | 0.08 | 0 | C |
| NGC1767=SL120 (in LH8=DEM36) | 50T | 10.61 | -0.58 | 0.24 | 2.15 | 0.05 | I | C |
| NGC1777=SL121=LW96 | 38C | 12.80 | 0.17 | 0.60 | 1.64 | -4.83 | IVB | C |
| NGC1768=SL127 | 50T | 12.79 | 0.31 | 0.72 | 2.23 | 1.20 | V | C |
| N92=LH11=DEM38 | 100T | 12.03 | -0.91 | -0.18 | 2.18 | 0.74 | 0 | NA |

TABLE 1—Continued

| NAME | D(°) | V | U-B | B-V | X(°) | Y(°) | SWB | TYPE |
|--|-------|-------|-------|-------|------|--------|-----|------|
| NGC1772=SL128 (in LH8=DEM36) | 72V | 10.97 | -0.56 | 0.25 | 2.10 | -0.11 | I | C |
| NGC1773=LH14=N11E=DEM41 (in N11,in N10) | 100T | 11.28 | -0.63 | 0.15 | 2.32 | 3.09 | I | NA |
| SL133=LW99 | 61C | 13.58 | 0.04 | 0.53 | 2.50 | 4.18 | IVA | C |
| NGC1775=SL129 | 72V | 12.55 | -0.06 | 0.35 | 2.00 | -0.98 | III | C |
| KMHK345 (in NGC1770=N91=SL130,in DEM39) | 150T | 9.63 | -0.85 | -0.02 | 2.18 | 1.04 | 0 | NA |
| KMHK341 (in NGC1770=N91=SL130,in DEM39) | 150T | 10.63 | -1.02 | -0.14 | 2.19 | 1.02 | 0 | NA |
| SL134 | 34T | 12.40 | -0.42 | 0.21 | 2.17 | 1.09 | I | C |
| SL142=LW105 | 24C | 14.51 | 0.02 | 0.28 | 2.42 | 4.06 | III | C |
| NGC1774=SL141 | 60V | 10.76 | -0.27 | 0.20 | 2.24 | 2.21 | II | C |
| NGC1782=SL140 (in LH8=DEM36) | 72V | 10.50 | -0.26 | 0.25 | 2.03 | 0.06 | II | C |
| NGC1776=SL145 (sup N10) | 50T | 13.01 | -0.07 | 0.27 | 2.27 | 3.02 | III | C |
| NGC1789=SL144=LW104 | 50T | 13.06 | 0.22 | 0.50 | 1.76 | -2.45 | IVB | C |
| NGC1783=SL148 (sup N10) | 72V | 10.93 | 0.23 | 0.61 | 2.26 | 3.45 | V | C |
| NGC1786=SL149 | 60V | 10.88 | 0.10 | 0.74 | 2.09 | 1.71 | VII | C |
| SL151 | 38C | 13.34 | 0.30 | 0.88 | 1.88 | -0.51 | VI | C |
| SL152=LW108 (sup DEM43) | 50T | 13.79 | -0.01 | 0.27 | 2.29 | 3.89 | III | C |
| SL153 (sup N10) | 50T | 12.03 | -0.15 | 0.23 | 2.21 | 3.13 | III | C |
| NGC1791=SL155 (in N186E=DEM50) | 50T | 13.12 | -0.23 | 0.33 | 1.84 | -0.72 | II | CA |
| SL158 | 50T | 11.90 | -0.44 | 0.01 | 1.82 | -0.80 | I | C |
| NGC1793=SL163 | 44V | 12.41 | -0.30 | 0.28 | 1.86 | -0.10 | I | C |
| SL164 | 50T | 13.49 | 0.30 | 0.66 | 1.67 | -2.10 | VI | C |
| NGC1795=SL165 | 100T | 12.42 | 0.27 | 0.73 | 1.82 | -0.35 | V | C |
| SL168=LW114 (sup DEM43) | 50T | 13.20 | 0.03 | 0.24 | 2.15 | 4.00 | III | C |
| NGC1801=SL170 | 62V | 12.16 | 0.09 | 0.27 | 1.77 | -0.16 | IVA | C |
| NGC1804=SL172 | 72V | 11.87 | -0.22 | 0.15 | 1.78 | 0.37 | II | C |
| SL174 | 50T | 13.39 | 0.36 | 0.62 | 1.89 | 1.64 | V | C |
| SL178=ESO85SC31 (in NGC1787=LH15,in DEM43) | 31V | 10.92 | -0.59 | 0.17 | 2.02 | 3.63 | I | C |
| SL180 | 38C | 13.49 | 0.18 | 0.66 | 1.77 | 0.46 | V | C |
| SL181 | 38C | 13.21 | 0.03 | 0.45 | 1.73 | 0.28 | IVA | C |
| SL188 | 50T | 12.40 | -0.26 | 0.42 | 1.70 | 0.68 | I | C |
| SL191 (in LH16) | 40T | 12.16 | -0.24 | 0.35 | 1.64 | 0.46 | I | C |
| NGC1805=SL186 | 60V | 10.63 | -0.55 | 0.11 | 1.93 | 3.34 | I | C |
| NGC1806=SL184 | 88V | 11.10 | 0.31 | 0.73 | 1.78 | 1.47 | V | C |
| NGC1815=SL189 (in DEM55) | 40T | 12.41 | -0.59 | 0.02 | 1.52 | -1.16 | I | C |
| NGC1810=SL194 | 72V | 11.90 | -0.51 | 0.22 | 1.80 | 3.07 | I | C |
| NGC1813=SL190 (in LH18) | 50T | 12.76 | -0.51 | 0.38 | 1.53 | -0.86 | I | C |
| SL197 | 38C | 13.77 | 0.16 | 0.59 | 1.68 | 1.83 | IVB | C |
| NGC1814=N17B (in N17,in NGC1820=SL199=LH19,in DEM59) | 40T | 12.76 | -0.98 | -0.18 | 1.69 | 2.16 | 0 | NA |
| NGC1816 (in NGC1820=SL199=LH19,in DEM59) | 40T | 13.02 | -0.79 | -0.14 | 1.68 | 2.20 | 0 | C |
| NGC1820=SL199=LH19 (in DEM59) | 150T | 11.50 | -0.88 | -0.15 | 1.66 | 2.19 | 0 | NA |
| NGC1818=SL201 | 72V | 9.70 | -0.46 | 0.18 | 1.72 | 3.02 | I | C |
| SL200 (in LH18) | 50T | 12.78 | -0.55 | 0.09 | 1.43 | -0.94 | I | AC |
| SL205 | 50T | 13.83 | 0.09 | 0.45 | 1.66 | 3.09 | IVA | C |
| NGC1833=SL206 (in N190=DEM63,in LH24) | 100T | 11.73 | -0.82 | -0.29 | 1.35 | -1.27 | 0 | NA |
| NGC1834=ESO56SC60 | 45V | 11.82 | -0.32 | 0.29 | 1.40 | 0.25 | I | C |
| NGC1835=SL215 | 62V | 10.17 | 0.13 | 0.73 | 1.39 | 0.06 | VII | C |
| NGC1822=SL210 | 50T | 13.15 | -0.23 | 0.09 | 1.64 | 3.25 | II | C |
| NGC1829=N23A=SL208 (in DEM66e,in N23) | 50T | 12.13 | -0.85 | -0.10 | 1.51 | 1.40 | 0 | NA |
| NGC1836=SL223 | 50T | 12.22 | 0.02 | 0.28 | 1.41 | 0.83 | III | C |
| LH23 | 150T | 11.53 | -1.04 | -0.11 | 1.34 | -1.43 | 0 | NA |
| N191A=DEM64b (in SL209,in LH23) | 40T | 12.43 | -1.03 | -0.15 | 1.31 | -1.45 | 0 | NC |
| SL212 | 100T | 12.20 | -0.24 | 0.18 | 1.49 | 0.94 | II | C |
| SL216 | 40T | 12.72 | -0.45 | -0.01 | 1.36 | -0.56 | I | C |
| SL218 | 100T | 12.24 | -0.34 | 0.13 | 1.47 | 0.99 | I | C |
| NGC1823=SL198 (in LH18) | 50T | 12.09 | -0.92 | -0.18 | 1.46 | -0.88 | 0 | CA |
| NGC1825=SL202 | 34T | 12.04 | -0.26 | 0.41 | 1.50 | 0.53 | I | C |
| NGC1826=SL221 | 50T | 13.25 | 0.20 | 0.53 | 1.59 | 3.23 | IVB | C |
| NGC1828=SL203 | 72V | 12.52 | -0.16 | 0.13 | 1.46 | 0.07 | III | C |
| NGC1830=SL207 | 72V | 12.56 | 0.13 | 0.19 | 1.44 | 0.12 | IVA | C |
| NGC1831=SL227=LW133 | 60V | 11.18 | 0.13 | 0.34 | 1.62 | 4.54 | IVB | C |
| NGC1837=SL217 (in LH24) | 100T | 10.63 | -0.81 | -0.14 | 1.31 | -1.26 | 0 | AC |
| NGC1838=SL225 (in DEM76) | 50T | 12.93 | -0.23 | 0.27 | 1.37 | 1.02 | II | C |
| NGC1839=SL226 | 50T | 11.80 | -0.18 | 0.10 | 1.37 | 0.83 | II | C |
| NGC1841=ESO4SC15 | 187TC | 11.43 | 0.15 | 0.80 | 0.73 | -14.56 | VII | C |
| HS109 | 50T | 12.52 | -0.26 | 0.11 | 1.42 | 0.78 | II | C |
| SL224 | 50T | 13.53 | 0.14 | 0.33 | 1.27 | -0.87 | IVA | C |
| SL229 (sup DEM76) | 50T | 13.28 | 0.24 | 0.33 | 1.39 | 1.11 | IVA | C |
| SL230 (in DEM76) | 50T | 11.34 | -0.35 | 0.29 | 1.38 | 1.13 | I | C |
| SL234 | 40T | 12.44 | -0.36 | -0.03 | 1.32 | 0.78 | II | C |
| SL237 (in LH27) | 50T | 11.27 | -0.16 | 0.42 | 1.28 | 0.34 | II | CA |
| SL244 (sup N100=DEM79) | 40T | 13.04 | 0.13 | 0.77 | 1.26 | 0.94 | VII | C |
| HS117 | 50T | 13.00 | 0.34 | 0.67 | 1.34 | 0.78 | V | C |
| NGC1842=SL241 | 38C | 14.02 | 0.08 | 0.31 | 1.35 | 2.19 | IVA | C |
| NGC1844=SL242 | 72V | 12.08 | -0.14 | 0.21 | 1.32 | 2.14 | III | C |
| NGC1845 (in LH26) | 150T | 10.20 | -0.58 | 0.31 | 1.24 | -1.07 | I | A |
| SL232 (in NGC1845,in LH26) | 50T | 12.74 | -0.28 | 0.23 | 1.21 | -1.02 | I | C |
| LW137 | 61C | 13.81 | 0.22 | 0.71 | 0.86 | -5.96 | V | C |
| NGC1846=SL243 | 62V | 11.31 | 0.31 | 0.77 | 1.31 | 2.00 | VI | C |
| NGC1847=SL240 | 72V | 11.06 | -0.33 | 0.20 | 1.24 | 0.49 | I | C |
| SL249 (sup DEM75) | 50T | 12.84 | 0.05 | 0.32 | 1.08 | -1.29 | IVA | C |
| SL250 | 34T | 13.15 | 0.21 | 0.59 | 1.17 | 0.04 | IVB | C |
| SL251 | 50T | 12.93 | -0.04 | 0.26 | 1.11 | -0.41 | III | C |
| SL255 (in LH29) | 50T | 12.54 | -0.22 | 0.20 | 1.10 | -0.59 | II | C |

TABLE 1—Continued

| NAME | D(‘) | V | U-B | B-V | X(°) | Y(°) | SWB | TYPE |
|---|------|-------|-------|-------|------|-------|-----|------|
| NGC1848=SL247 (in DEM81,in LH28) | 150T | 9.73 | -0.43 | 0.05 | 1.06 | -1.73 | I | AN |
| SL256 (in LH28) | 40T | 12.45 | -0.35 | 0.22 | 1.01 | -1.71 | I | C |
| SL260 | 38C | 13.15 | -0.06 | 0.34 | 1.15 | 0.79 | III | C |
| SL262=LW146=ESO119SC40 | 38C | 14.25 | 0.06 | 0.73 | 1.44 | 7.08 | VII | C |
| SL268 | 50T | 12.16 | 0.33 | 0.66 | 1.04 | -0.11 | V | C |
| SL276 | 40T | 12.95 | 0.19 | 0.45 | 1.00 | 0.13 | IVB | C |
| NGC1849=SL267 | 50T | 12.77 | 0.11 | 0.31 | 1.18 | 3.15 | IVA | C |
| Rob1=NGC1850A (in N103B) | 25T | 11.23 | -0.89 | -0.14 | 1.13 | 0.70 | 0 | C |
| NGC1850=SL261=BRHT5a (in ? N103B) | 50T | 9.57 | -0.27 | 0.15 | 1.11 | 0.70 | II | C |
| H88-159=BRHT5b (in ? N103B) | 40T | 11.84 | -0.41 | 0.14 | 1.08 | 0.69 | I | C |
| NGC1852=SL264 | 72V | 12.01 | 0.25 | 0.73 | 1.11 | 1.69 | V | C |
| NGC1854=NGC1855=SL265 | 72V | 10.39 | -0.27 | 0.19 | 1.06 | 0.62 | II | C |
| NGC1856=SL271 | 62V | 10.06 | 0.10 | 0.35 | 1.02 | 0.34 | IVA | C |
| NGC1858=N105A=SL274=LH31 (in N105=DEM86) | 150T | 9.88 | -0.90 | -0.12 | 1.00 | 0.57 | 0 | NA |
| SL278 (sup DEM88) | 38C | 13.63 | -0.02 | 0.50 | 1.02 | 0.99 | IVA | C |
| SL280 | 150T | 11.92 | -0.61 | 0.27 | 0.97 | 0.14 | I | C |
| SL288 | 34T | 12.06 | -0.40 | -0.03 | 0.94 | 0.44 | I | C |
| SL291 | 50T | 13.26 | 0.26 | 0.51 | 0.83 | -1.44 | IVB | C |
| SL296 | 34T | 13.10 | 0.12 | 0.42 | 0.89 | -0.09 | IVA | C |
| NGC1859=SL297=LW156 | 100T | 12.10 | -0.09 | 0.43 | 1.04 | 4.22 | III | C |
| NGC1860=SL284 | 72V | 11.04 | -0.39 | 0.14 | 0.94 | 0.71 | I | C |
| NGC1861=SL286 | 50T | 13.16 | 0.21 | 0.47 | 0.85 | -1.31 | IVB | C |
| SL298 | 50T | 13.18 | 0.23 | 0.56 | 0.96 | 2.49 | IVB | C |
| SL302 | 50T | 13.31 | 0.13 | 0.44 | 0.78 | -0.60 | IVA | C |
| SL304 | 40T | 12.99 | -0.05 | 0.33 | 0.82 | 0.28 | III | C |
| NGC1862=SL306 | 50T | 13.33 | -0.15 | 0.18 | 0.89 | 3.31 | III | C |
| NGC1863=SL299 | 72V | 10.98 | -0.33 | 0.16 | 0.85 | 0.74 | I | C |
| SL308 | 50T | 13.50 | -0.04 | 0.15 | 0.80 | 1.17 | III | C |
| SL328=LH39 (in DEM110) | 100T | 10.86 | -0.74 | 0.03 | 0.65 | -0.06 | I | A |
| NGC1864=SL309 | 50T | 12.86 | -0.10 | 0.19 | 0.81 | 1.84 | III | C |
| NGC1865=SL307 | 40T | 12.91 | 0.08 | 0.69 | 0.78 | 0.70 | VII | C |
| NGC1866=SL319=LW163 | 72V | 9.73 | -0.02 | 0.25 | 0.81 | 4.00 | III | C |
| NGC1867=SL321 | 50T | 13.35 | 0.12 | 0.45 | 0.77 | 3.18 | IVA | C |
| NGC1868=SL330=LW169 | 62V | 11.57 | 0.15 | 0.45 | 0.77 | 5.52 | IVA | C |
| NGC1869=SL326=LH37 (in DEM105,in N30) | 150T | 10.46 | -0.68 | 0.15 | 0.70 | 2.09 | I | AN |
| NGC1870=SL317 | 72V | 11.26 | -0.21 | 0.19 | 0.70 | 0.35 | II | C |
| NGC1871=SL325=LH38 (in N30C=DEM106) | 150T | 10.09 | -0.64 | 0.12 | 0.72 | 2.03 | I | AN |
| NGC1872=SL318 (sup N113) | 60V | 11.04 | 0.06 | 0.35 | 0.69 | 0.16 | IVA | C |
| NGC1873=SL324=LH36 (in DEM105,in N30) | 150T | 10.44 | -0.83 | -0.09 | 0.71 | 2.13 | 0 | AN |
| NGC1874=N113D (in SL320,in DEM104,in N113=LH35) | 50T | 12.81 | -1.03 | -0.34 | 0.68 | 0.10 | 0 | NA |
| NGC1876=N113C (in SL320,in DEM104,in N113=LH35) | 50T | 11.71 | -1.00 | -0.17 | 0.68 | 0.12 | 0 | NA |
| SL320 (in DEM104,in N113=LH35) | 150T | 10.34 | -1.02 | -0.20 | 0.67 | 0.11 | 0 | NA |
| NGC1878=SL316 | 50T | 12.94 | 0.07 | 0.29 | 0.66 | -1.00 | IVA | C |
| NGC1882=SL340 | 150T | 12.33 | -0.11 | 0.10 | 0.59 | 3.34 | III | C |
| NGC1885=SL338 | 72V | 11.97 | -0.05 | 0.38 | 0.53 | 0.49 | III | C |
| SL337=LW173 | 38C | 13.28 | 0.04 | 0.37 | 0.42 | -3.64 | IVA | C |
| SL339 | 38C | 13.87 | 0.07 | 0.47 | 0.54 | 1.18 | IVA | C |
| SL349 | 50T | 13.27 | 0.34 | 0.62 | 0.40 | 0.64 | V | C |
| SL352 | 50T | 13.12 | 0.20 | 0.41 | 0.34 | -1.07 | IVA | C |
| H1=SL353 | 50T | 12.40 | 0.27 | 0.66 | 0.38 | 0.64 | V | C |
| NGC1887=SL343 | 50T | 12.72 | -0.17 | 0.19 | 0.53 | 3.15 | II | C |
| NGC1890=SL331=LW167 | 61C | 12.81 | -0.25 | 0.27 | 0.52 | -2.61 | II | C |
| NGC1894=SL344 | 34T | 12.16 | -0.21 | 0.24 | 0.45 | 0.00 | II | C |
| NGC1895=N33=DEM121 | 100T | 12.93 | -1.03 | -0.28 | 0.42 | 2.14 | 0 | NA |
| SL354=LW177 | 61C | 13.65 | 0.13 | 0.78 | 0.46 | 6.05 | VII | C |
| SL357 | 38C | 13.30 | 0.29 | 0.64 | 0.34 | 0.14 | V | C |
| SL358 | 40T | 13.10 | 0.09 | 0.40 | 0.32 | -0.01 | IVA | C |
| SL359 | 61C | 13.74 | 0.03 | 0.61 | 0.30 | 1.00 | VII | C |
| NGC1897=SL355 | 50T | 13.49 | 0.18 | 0.36 | 0.35 | 2.03 | IVA | C |
| NGC1898=SL350 | 40T | 11.86 | 0.08 | 0.76 | 0.37 | -0.18 | VII | C |
| SL362 | 50T | 11.48 | -0.75 | 0.11 | 0.31 | -0.06 | I | C |
| H2=SL363 | 62VT | 11.90 | 0.23 | 0.60 | 0.30 | -0.13 | V | C |
| NGC1900=SL376=LW184 | 38C | 13.59 | 0.11 | 0.36 | 0.29 | 6.45 | IVA | C |
| NGC1902=SL367 | 50T | 11.77 | -0.19 | 0.27 | 0.30 | 2.85 | II | C |
| NGC1903=SL356 (sup ? DEM130) | 60V | 11.86 | -0.25 | 0.14 | 0.32 | 0.14 | II | C |
| NGC1905=SL369 | 50T | 13.21 | 0.08 | 0.25 | 0.28 | 2.20 | IVA | C |
| H88-266 (in LH41=DEM132,in N119) | 100T | 10.98 | -0.86 | -0.06 | 0.27 | 0.21 | 0 | C |
| H88-267=SDorCluster (in LH41=DEM132,in N119) | 100T | 9.09 | -0.69 | 0.11 | 0.25 | 0.24 | I | C |
| SL360 (in LH41=DEM132,in N119) | 100T | 9.54 | -0.91 | -0.15 | 0.27 | 0.26 | 0 | C |
| NGC1910=SL371 (in LH41=DEM132,in N119) | 150T | 9.65 | -0.88 | -0.15 | 0.20 | 0.24 | 0 | NA |
| NGC1913=SL373 | 62V | 11.14 | -0.20 | 0.23 | 0.23 | -0.06 | II | C |
| NGC1914=SL365=LH40 (in N195=DEM131) | 100T | 12.01 | -0.96 | -0.15 | 0.24 | -1.78 | 0 | NA |
| NGC1916=SL361 (sup DEM130) | 44V | 10.38 | 0.18 | 0.78 | 0.21 | 0.07 | VII | C |
| NGC1917=SL379 | 50T | 12.33 | 0.20 | 0.57 | 0.18 | 0.48 | IVB | C |
| NGC1918=N120=LH42=DEM134 | 150T | 9.78 | -0.93 | 0.03 | 0.16 | -0.17 | 0 | NA |
| SL364 | 50T | 13.21 | -0.19 | 0.29 | 0.24 | -1.59 | II | C |
| SL368 | 50T | 13.03 | 0.22 | 0.52 | 0.28 | -0.44 | IVB | C |
| SL378 | 100T | 13.11 | -0.02 | 0.34 | 0.20 | 1.26 | III | C |
| SL382 | 100T | 13.33 | -0.47 | 0.09 | 0.19 | 2.98 | I | C |
| SL383 | 50T | 12.65 | -0.16 | 0.27 | 0.14 | 1.20 | III | C |
| SL385 | 40T | 12.78 | 0.07 | 0.37 | 0.16 | -0.03 | IVA | C |
| SL386 | 24C | 13.32 | -0.19 | 0.23 | 0.17 | 4.09 | II | C |
| SL387 | 40T | 13.07 | 0.08 | 0.44 | 0.14 | -0.01 | IVA | C |

TABLE 1—Continued

| NAME | D('') | V | U-B | B-V | X($^{\circ}$) | Y($^{\circ}$) | SWB | TYPE |
|---|-------|-------|-------|-------|-----------------|-----------------|-----|------|
| SL388=LW186 | 38C | 13.85 | 0.13 | 0.73 | 0.18 | 6.00 | VII | C |
| SL390 | 100T | 12.53 | -0.03 | 0.52 | 0.13 | 0.56 | IVA | C |
| SL393=ESO56SC103 | 38C | 12.61 | -0.43 | 0.41 | 0.12 | 0.08 | I | C |
| SL396=LW187 | 38C | 13.56 | 0.23 | 0.86 | 0.05 | -3.63 | VI | C |
| NGC1920=N38 (in DEM138) | 100T | 12.54 | -0.92 | -0.20 | 0.08 | 2.70 | 0 | NC |
| NGC1921w=N121=BRHT49b (in DEM133) | 34T | 13.21 | -0.81 | 0.02 | 0.12 | -0.31 | 0 | NC |
| NGC1921e=SL381=BRHT49a (in DEM133) | 34T | 12.95 | -0.21 | 0.19 | 0.14 | -0.31 | II | C |
| NGC1922=SL391 | 34T | 11.51 | -0.41 | 0.13 | 0.10 | 0.03 | I | C |
| SL397 | 34T | 12.22 | -0.37 | 0.12 | 0.10 | 0.61 | I | C |
| SL398=LW189 | 24C | 13.72 | 0.00 | 0.40 | 0.07 | 4.18 | IVA | C |
| LH43 (in DEM137) | 150T | 11.24 | -0.89 | 0.25 | 0.03 | 4.02 | I | A |
| NGC1923=SL404=N40=DEM137a (in DEM137) | 50T | 12.95 | -0.91 | -0.04 | -0.01 | 3.99 | 0 | NC |
| NGC1925n=N43=LH45nw=DEM155 | 150T | 9.85 | -0.84 | 0.09 | -0.04 | 3.71 | 0 | NA |
| NGC1925s=LH45s (in DEM154) | 150T | 10.98 | -0.66 | 0.50 | -0.04 | 3.67 | I | A |
| NGC1926=SL403 | 40T | 11.79 | -0.09 | 0.26 | 0.03 | -0.05 | III | C |
| NGC1928=SL405=HS243 | 34T | 12.47 | 0.07 | 0.71 | 0.00 | 0.00 | VII | C |
| SL410=LW192 | 61C | 12.16 | 0.07 | 0.27 | -0.03 | 4.25 | IVA | C |
| BCD1 (in LH46) | 40T | 13.49 | -0.94 | -0.22 | -0.03 | 0.08 | 0 | C |
| SL411 | 38C | 13.83 | -0.45 | -0.03 | -0.05 | 1.80 | I | C |
| SL412 | 40T | 13.17 | -0.09 | 0.30 | -0.02 | -0.31 | III | C |
| SL418 | 40T | 12.82 | -0.06 | 0.19 | -0.05 | -0.13 | III | C |
| SL419 | 40T | 12.70 | 0.00 | 0.23 | -0.07 | 0.28 | III | C |
| HS248 (in N127A) | 50T | 12.70 | -1.04 | -0.25 | -0.05 | -0.18 | 0 | NC |
| SL423 | 40T | 12.69 | -0.24 | 0.13 | -0.09 | 0.01 | II | C |
| NGC1932=SL420 | 40T | 11.84 | -0.18 | 0.30 | -0.11 | 3.33 | II | C |
| NGC1929=N44F=DEM151a (in SL417,in LH47,in N44) | 50T | 12.42 | -1.02 | -0.23 | -0.04 | 1.57 | 0 | NA |
| NGC1934 (in SL417,in LH47=DEM152,in N44) | 150T | 10.50 | -0.94 | -0.15 | -0.06 | 1.54 | 0 | NA |
| NGC1935=IC2126=N44B (in SL417,in LH47,in N44) | 50T | 11.23 | -0.98 | -0.17 | -0.08 | 1.52 | 0 | NC |
| NGC1936=IC2127=N44C (in SL417,in LH47,in N44) | 50T | 11.60 | -0.53 | -0.08 | -0.10 | 1.50 | 0 | NC |
| SL417P1 (in LH47=DEM152,in N44) | 150T | 9.89 | -0.95 | -0.16 | -0.08 | 1.53 | 0 | NA |
| BCDSP2 (in LH47=DEM152,in N44) | 150T | 10.18 | -0.91 | -0.12 | -0.11 | 1.52 | 0 | NA |
| N44D=SL429 (in IC2128=LH49=DEM160,in N44) | 100T | 11.10 | -1.09 | -0.18 | -0.16 | 1.41 | 0 | NC |
| N44K (in DEM158,in N44) | 50T | 13.25 | -0.96 | -0.03 | -0.11 | 1.41 | 0 | NA |
| SL424 | 40T | 13.15 | 0.05 | 0.36 | -0.12 | 1.32 | IVA | C |
| NGC1937=N44I=SL422=LH48=DEM156 (in N44) | 150T | 10.37 | -0.80 | 0.08 | -0.12 | 1.59 | 0 | NA |
| SL425 | 100T | 12.52 | -0.28 | 0.30 | -0.10 | 0.74 | I | C |
| NGC1938=SL413 | 38CT | 13.09 | 0.05 | 0.47 | -0.04 | -0.46 | IVA | C |
| NGC1939=SL414 | 38CT | 11.78 | 0.09 | 0.69 | -0.06 | -0.48 | VII | C |
| NGC1940=SL427 | 50T | 11.91 | -0.19 | 0.30 | -0.14 | 2.29 | II | C |
| SL431 | 50T | 12.95 | -0.12 | 0.25 | -0.15 | -0.78 | III | C |
| NGC1941=N46 (in DEM162) | 100T | 12.00 | -0.76 | 0.07 | -0.17 | 3.10 | I | NC |
| SL446 | 100T | 13.45 | 0.17 | 0.82 | -0.34 | 1.76 | VII | C |
| NGC1942=SL445=LW203 | 61C | 13.46 | 0.21 | 0.78 | -0.34 | 5.54 | VI | C |
| NGC1943=SL430 | 60V | 11.88 | -0.17 | 0.27 | -0.14 | -0.68 | II | C |
| NGC1944=SL426=LW194 | 61C | 11.84 | 0.01 | 0.27 | -0.12 | -3.01 | III | C |
| IC2134=SL437=LW198 | 38C | 13.94 | 0.15 | 0.79 | -0.22 | -5.97 | VII | C |
| SL451=LW206 | 38C | 14.20 | 0.18 | 0.80 | -0.29 | -6.08 | VII | C |
| BCDSP3 (includes SL452=KMHK871) | 187T | 11.78 | -0.26 | 0.35 | -0.38 | 2.83 | I | A |
| SL453 | 40T | 12.27 | -0.05 | 0.30 | -0.32 | 0.11 | III | C |
| SL455=LW207 | 61C | 14.12 | 0.29 | 0.60 | -0.29 | -6.73 | VI | C |
| NGC1946=SL454 (in NGC1945,in N48) | 50T | 12.62 | -0.43 | 0.04 | -0.39 | 3.09 | I | C |
| NGC1948=SL458=LH52=DEM189 (in N48) | 150T | 10.61 | -0.66 | 0.20 | -0.44 | 3.22 | I | NA |
| N49=DEM190=SNR525-66.1 (in LH53) | 100T | 12.71 | -1.16 | -0.17 | -0.47 | 3.39 | 0 | SNR |
| NGC1949=N138A (in DEM180) | 50T | 12.39 | -0.87 | -0.22 | -0.37 | 1.01 | 0 | NC |
| NGC1950=SL450 | 40T | 13.17 | 0.22 | 0.54 | -0.32 | -0.42 | IVB | C |
| NGC1951=SL464 | 60V | 10.58 | -0.19 | 0.09 | -0.47 | 2.89 | II | C |
| NGC1953=SL459 | 62V | 11.74 | 0.07 | 0.23 | -0.40 | 0.65 | III | C |
| SL456=LH51 (in N51D=DEM192,in N51) | 100T | 11.75 | -1.02 | -0.23 | -0.41 | 2.01 | 0 | NA |
| SL465 | 100T | 12.57 | -0.41 | 0.15 | -0.49 | 2.82 | I | C |
| SL468 | 40T | 12.42 | -0.13 | 0.15 | -0.42 | 0.03 | III | C |
| SL463=LW213 (in LH53) | 100T | 12.27 | -0.28 | 0.19 | -0.49 | 3.43 | II | C |
| NGC1955=SL467=LH54 (in N51D=DEM192,in N51) | 150T | 9.83 | -1.00 | -0.21 | -0.46 | 1.99 | 0 | NA |
| SL470 (in DEM195) | 50T | 12.45 | -0.44 | 0.09 | -0.51 | 3.10 | I | C |
| SL471 (in N51E=LH55=DEM196,in N51) | 100T | 11.73 | -1.02 | -0.22 | -0.48 | 1.86 | 0 | NA |
| SL475=LH57 (in N143) | 100T | 11.52 | -0.93 | -0.20 | -0.46 | 0.23 | 0 | NA |
| SL428=LW196 (in DEM155a,in NGC1925n=N43=DEM155) | 100T | 12.71 | -1.00 | -0.33 | -0.15 | 3.77 | 0 | CN |
| HS298 | 25T | 12.59 | -0.53 | 0.47 | -0.47 | -0.01 | I | C |
| NGC1958=SL462 | 34T | 12.99 | 0.03 | 0.54 | -0.40 | -0.35 | IVA | C |
| NGC1959=SL466 | 34T | 12.17 | -0.03 | 0.38 | -0.41 | -0.44 | IVA | C |
| NGC1962 (in SL476=LH58,in N144=DEM199) | 100T | 11.47 | -0.95 | -0.27 | -0.47 | 0.65 | 0 | NA |
| NGC1965 (in SL476=LH58,in N144=DEM199) | 50T | 11.70 | -0.92 | -0.18 | -0.49 | 0.68 | 0 | NC |
| NGC1966=N144A (in SL476=LH58,in N144=DEM199) | 50T | 11.83 | -0.89 | -0.23 | -0.52 | 0.67 | 0 | NC |
| NGC1967=SL478 (in DEM198) | 50T | 10.83 | -0.75 | 0.05 | -0.51 | 0.38 | I | C |
| SL477 | 45V | 12.70 | -0.35 | 0.07 | -0.46 | -2.21 | II | C |
| HS301A | 40T | 12.50 | 0.04 | 0.43 | -0.48 | -2.50 | IVA | C |
| NGC1968w=SL483w=LH60w (in DEM201,in N51) | 150T | 10.78 | -0.96 | -0.04 | -0.62 | 2.03 | 0 | NA |
| NGC1968e=SL483e=LH60e (in DEM201,in N51) | 150T | 10.20 | -1.06 | -0.21 | -0.60 | 2.03 | 0 | NA |
| NGC1969=SL479 (in LH59) | 40T | 12.46 | -0.15 | 0.20 | -0.49 | -0.36 | III | C |
| NGC1970 (in SL476=LH58,in N144=DEM199) | 50T | 10.28 | -0.72 | 0.15 | -0.53 | 0.65 | I | NA |
| NGC1971=SL481 (in LH59) | 34T | 11.90 | -0.26 | 0.11 | -0.51 | -0.37 | II | C |
| SL482 | 100T | 11.59 | -0.71 | 0.05 | -0.60 | 3.12 | I | C |
| NGC1972=SL480 (in LH59) | 34T | 12.62 | -0.20 | 0.33 | -0.51 | -0.35 | II | C |
| SL485+BRHT36b | 150T | 11.67 | -0.39 | 0.24 | -0.65 | 3.46 | I | CA |

TABLE 1—Continued

| NAME | D(°) | V | U-B | B-V | X(°) | Y(°) | SWB | TYPE |
|--|------|-------|-------|-------|-------|-------|-----|------|
| NGC1974=N51A=SL494=LH63 (in N51) | 150T | 10.30 | -0.97 | -0.21 | -0.65 | 2.06 | 0 | NA |
| SL490=LW217 | 61T | 13.90 | 0.22 | 0.82 | -0.51 | -4.19 | VI | C |
| SL495 | 40T | 11.65 | -0.43 | 0.05 | -0.63 | 0.67 | I | C |
| HS314 (in DEM210) | 50T | 11.62 | -0.75 | -0.11 | -0.64 | 0.53 | 0 | C |
| BCDSP4 (sup ? DEM211) | 150T | 12.20 | -0.11 | 0.22 | -0.68 | 1.85 | III | A |
| SL498 (in DEM212) | 50T | 12.01 | -0.69 | -0.01 | -0.71 | 2.26 | 0 | C |
| NGC1978=SL501 | 62V | 10.70 | 0.25 | 0.78 | -0.74 | 3.25 | VI | C |
| NGC1983=LH61 (in DEM210) | 150T | 8.84 | -0.75 | 0.16 | -0.57 | 0.53 | I | AN |
| SL492 (in NGC1983=LH61,in DEM210) | 50T | 9.94 | -0.70 | 0.16 | -0.60 | 0.50 | I | C |
| NGC1984=SL488 (in DEM210) | 50T | 9.99 | -0.82 | 0.01 | -0.60 | 0.35 | 0 | C |
| NGC1986=SL489 | 60V | 11.07 | -0.20 | 0.24 | -0.58 | -0.49 | II | C |
| NGC1987=SL486 | 62V | 12.08 | 0.23 | 0.54 | -0.54 | -1.25 | IVB | C |
| NGC1994=SL499 (in DEM210) | 50T | 9.78 | -0.69 | 0.09 | -0.66 | 0.35 | I | C |
| HS319 (sup DEM210) | 40T | 12.50 | 0.08 | 0.33 | -0.69 | 0.53 | IVA | C |
| SL503 (sup DEM203) | 38C | 13.74 | -0.02 | 0.40 | -0.73 | 1.07 | IVA | C |
| SL502 | 100T | 11.36 | -0.51 | 0.06 | -0.78 | 2.90 | I | C |
| SL505 | 150T | 12.64 | 0.17 | 0.78 | -0.65 | -2.15 | VII | C |
| SL508 | 40T | 11.92 | -0.25 | 0.21 | -0.70 | -0.06 | II | C |
| SL509=LW221 | 61C | 13.23 | 0.19 | 0.73 | -0.91 | 5.84 | VII | C |
| SL513 | 50T | 12.41 | -0.74 | -0.11 | -0.85 | 2.73 | 0 | C |
| SL515=LW223 | 61C | 13.75 | -0.03 | 0.59 | -0.95 | 6.06 | IVA | C |
| ESO86SC2=KMHK981 | 150T | 11.13 | -0.35 | 0.31 | -0.92 | 3.58 | I | AC |
| SL516 (in DEM214) | 50T | 12.14 | -0.61 | -0.05 | -0.85 | 2.51 | 0 | CN |
| SL522 | 50T | 12.10 | -0.78 | -0.09 | -0.91 | 2.30 | 0 | C |
| SL524 | 100T | 12.52 | -0.51 | -0.08 | -0.95 | 3.16 | I | C |
| H14=SL506=LW220 | 62V | 13.42 | 0.21 | 0.72 | -0.60 | -4.14 | V | C |
| SL528 | 40T | 13.32 | 0.29 | 0.52 | -0.79 | -0.73 | IVB | C |
| LH65 (in DEM214) | 150T | 10.59 | -0.82 | 0.33 | -0.84 | 1.57 | I | AN |
| NGC1997=SL520=LW226 | 61C | 13.43 | 0.16 | 0.84 | -1.00 | 6.29 | VII | C |
| NGC2000=SL493 | 50T | 12.14 | -0.20 | 0.18 | -0.54 | -2.39 | II | C |
| NGC2001sw=SL507sw=LH64sw | 150T | 10.49 | -0.67 | 0.25 | -0.72 | 0.71 | I | A |
| NGC2001ne=SL507ne=LH64ne | 150T | 10.07 | -0.85 | -0.05 | -0.74 | 0.74 | 0 | A |
| NGC2002=SL517 (in LH77) | 50T | 10.10 | -0.58 | 0.34 | -0.89 | 2.61 | I | C |
| KMHK987 (in LH77) | 50T | 12.32 | -0.73 | -0.12 | -0.91 | 2.59 | 0 | C |
| SL529=LW229 | 38C | 13.66 | 0.25 | 0.73 | -1.05 | 5.95 | V | C |
| SL535 | 40T | 13.20 | -0.31 | 0.04 | -0.84 | -0.44 | II | C |
| NGC2003=SL526 | 40T | 11.30 | -0.55 | 0.05 | -0.95 | 3.02 | I | C |
| NGC2004=SL523 | 72V | 9.60 | -0.71 | 0.13 | -0.91 | 2.20 | I | C |
| NGC2005=SL518 | 25V | 11.57 | 0.20 | 0.73 | -0.80 | -0.26 | VII | C |
| SL536 | 50T | 13.02 | -0.38 | 0.17 | -0.79 | -2.32 | I | CA |
| NGC2006=SL537 (in LH77) | 50T | 10.88 | -0.63 | 0.12 | -0.98 | 2.52 | I | C |
| SL538 (in LH77) | 50T | 11.30 | -0.67 | -0.01 | -0.98 | 2.53 | 0 | C |
| SL539 | 45V | 11.03 | -0.13 | 0.17 | -0.84 | -1.21 | III | C |
| SL542 | 40T | 12.59 | -0.02 | 0.43 | -0.84 | -0.71 | IVA | C |
| SL543 | 50T | 12.23 | -0.12 | 0.18 | -0.82 | -2.40 | III | C |
| KMHK1019 (in LH77) | 40T | 11.49 | -0.57 | 0.48 | -1.03 | 2.49 | I | C |
| NGC2009=SL534 | 72V | 11.02 | -0.64 | 0.27 | -0.89 | 0.31 | I | C |
| LH70 | 150T | 10.70 | -0.68 | 0.25 | -1.03 | 2.13 | I | A |
| SL549 | 38C | 13.61 | 0.20 | 0.76 | -1.14 | 5.25 | VII | C |
| H4=SL556=LW237 | 38C | 13.33 | 0.16 | 0.66 | -1.16 | 4.76 | V | C |
| NGC2010=SL531 | 100T | 11.72 | -0.07 | 0.24 | -0.81 | -1.33 | III | C |
| HS346 (sup DEM224) | 34T | 12.83 | -0.11 | 0.27 | -0.97 | 0.13 | III | C |
| NGC2011=SL559=BRHT14a=KMHK1039 (in LH75) | 40T | 10.58 | -0.71 | 0.04 | -1.06 | 1.98 | I | C |
| BRHT14b=KMHK1040 (in LH75) | 40T | 12.02 | -0.70 | 0.37 | -1.06 | 1.95 | I | C |
| BCDSP5 (in DEM220) | 150T | 11.64 | -0.54 | -0.06 | -1.06 | 3.36 | 0 | A |
| NGC2014=SL560=LH76 (in N57,in N56) | 150T | 8.97 | -0.83 | 0.20 | -1.06 | 1.80 | 0 | NA |
| BCDSP6 (in NGC2014,in N57,in N56) | 34T | 11.41 | -0.99 | -0.19 | -1.04 | 1.80 | 0 | NC |
| SL551 | 100T | 13.25 | -0.30 | 0.05 | -1.00 | 1.50 | II | C |
| N148C=LH71 (in DEM227) | 150T | 10.11 | -0.87 | -0.05 | -0.98 | 0.96 | 0 | NA |
| BCDSP7 (in N148C=LH71,in DEM227) | 34T | 12.97 | -0.75 | 0.00 | -0.97 | 0.95 | 0 | CN |
| NGC2015=LH74 (in DEM224) | 150T | 10.43 | -0.66 | 0.13 | -0.99 | 0.25 | I | AN |
| SL553n (in N55=LH72,in DEM228) | 150T | 11.27 | -1.00 | -0.18 | -1.09 | 3.09 | 0 | NA |
| SL553s (in N55=LH72,in DEM228) | 150T | 10.42 | -1.07 | -0.20 | -1.11 | 3.03 | 0 | NA |
| SL555=LW236 | 61C | 13.06 | 0.18 | 0.77 | -0.86 | -2.65 | VII | C |
| LH69P1 (in N206=DEM221) | 150T | 10.20 | -0.83 | -0.02 | -0.82 | -1.58 | 0 | NA |
| NGC2018=N206A=SL533 (in LH69,in N206=DEM221) | 150T | 10.20 | -0.62 | -0.10 | -0.85 | -1.58 | 0 | NA |
| SL558 (sup DEM224) | 40T | 13.12 | 0.04 | 0.18 | -0.95 | 0.04 | III | C |
| SL562 | 50T | 12.43 | -0.09 | 0.11 | -0.92 | -1.76 | III | C |
| SL563 (in DEM224) | 50T | 12.54 | -0.64 | 0.02 | -0.97 | 0.13 | I | C |
| SL564 | 50T | 11.85 | -0.76 | -0.11 | -1.12 | 2.15 | 0 | C |
| SL566 | 50T | 12.62 | -0.02 | 0.24 | -1.00 | -1.29 | III | C |
| NGC2019=SL554 | 72V | 10.86 | 0.16 | 0.76 | -0.94 | -0.67 | VII | C |
| NGC2021=SL570 (in LH79,in DEM234) | 50T | 12.06 | -0.77 | -0.13 | -1.18 | 2.04 | 0 | C |
| LH77P1 | 187T | 10.55 | -0.64 | 0.19 | -0.97 | 2.47 | I | A |
| LH77P2 | 187T | 10.09 | -0.65 | 0.10 | -1.26 | 2.49 | I | A |
| LH77P3 | 187T | 10.39 | -0.73 | 0.04 | -1.09 | 2.51 | I | A |
| NGC2025=SL571 | 72V | 10.94 | -0.07 | 0.24 | -0.94 | -2.22 | III | C |
| NGC2027=SL592 (in LH84,LH77) | 100T | 10.97 | -0.89 | 0.00 | -1.34 | 2.58 | 0 | CA |
| SL567 (in LH78,in DEM234,in N56) | 150T | 10.19 | -0.83 | 0.09 | -1.15 | 1.97 | 0 | A |
| H3=SL569 | 40TC | 13.42 | 0.47 | 0.91 | -1.13 | 1.34 | VI | C |
| SL573=LW240 | 38C | 13.57 | 0.24 | 0.77 | -1.29 | 4.56 | VI | C |
| SL574 (in LH80) | 40T | 12.81 | -0.14 | 0.23 | -1.06 | -0.44 | III | C |
| SL576=LW239 | 61C | 13.68 | 0.08 | 0.38 | -0.90 | -4.88 | IVA | C |
| SL580 | 50T | 13.62 | 0.11 | 0.24 | -1.20 | 0.90 | IVA | C |
| KMHK1074 (in LH77) | 40T | 12.61 | -0.80 | -0.15 | -1.24 | 2.49 | 0 | C |

TABLE 1—Continued

| NAME | D(‘) | V | U-B | B-V | X(°) | Y(°) | SWB | TYPE |
|--|-------|-------|-------|-------|-------|-------|-----|------|
| SL583 | 50T | 13.33 | -0.05 | 0.27 | -1.21 | 0.95 | III | C |
| HS359 | 40T | 13.15 | 0.33 | 0.77 | -1.19 | 0.13 | VI | C |
| NGC2028=SL575 (in LH80) | 40T | 12.88 | 0.04 | 0.28 | -1.11 | -0.46 | III | C |
| SL579 | 61C | 12.80 | -0.42 | 0.17 | -1.23 | 1.64 | I | C |
| NGC2029 (in LH82,in N59) | 100T | 12.29 | -0.68 | -0.39 | -1.32 | 1.94 | 0 | NA |
| SL585=BRHT39a=KMHK1099 (sup DEM232e) | 40TC | 12.84 | -0.10 | 0.40 | -1.22 | 0.65 | III | C |
| IC2140=SL581=LW241 | 61C | 13.48 | 0.22 | 0.73 | -0.87 | -5.88 | V | C |
| SL586=ESO86SC12 (in LH77) | 40T | 11.17 | -0.80 | -0.12 | -1.31 | 2.53 | 0 | C |
| SL588 (sup DEM268) | 61C | 13.33 | 0.08 | 0.39 | -1.25 | 1.19 | IVA | C |
| SL591 | 40T | 12.88 | -0.10 | 0.30 | -1.17 | -0.39 | III | C |
| NGC2030=SL595 (in N63s=LH83,in DEM243,in N63) | 150T | 10.54 | -0.96 | -0.18 | -1.45 | 3.46 | 0 | NC |
| NGC2031=SL577 | 72V | 10.83 | -0.07 | 0.26 | -1.06 | -1.49 | III | C |
| NGC2032=N59Anw (in LH82,in N59) | 100T | 10.80 | -0.58 | -0.19 | -1.35 | 1.93 | 0 | NA |
| BCDSP8 (in NGC2033=SL589=LH81,in N154=DEM246) | 40T | 11.63 | -0.91 | -0.10 | -1.19 | -0.25 | 0 | CN |
| LH85 | 150T | 10.71 | -0.70 | 0.31 | -1.30 | 0.64 | I | AN |
| NGC2034n (in LH84,in LH77) | 150T | 9.78 | -0.58 | 0.29 | -1.41 | 2.62 | I | A |
| NGC2034s (in LH84,in LH77) | 150T | 10.35 | -0.75 | 0.24 | -1.39 | 2.58 | I | A |
| NGC2035=N59A (in LH82,in N59) | 100T | 10.99 | -0.76 | -0.17 | -1.37 | 1.91 | 0 | NA |
| NGC2036=SL587 | 40T | 12.77 | -0.10 | 0.19 | -1.17 | -0.57 | III | C |
| NGC2037 (in NGC2033=SL589=LH81,in N154=DEM246) | 150T | 10.31 | -0.83 | -0.10 | -1.22 | -0.24 | 0 | NA |
| NGC2038=SL590 | 40T | 11.92 | -0.21 | 0.18 | -1.16 | -1.07 | II | C |
| NGC2040=N59B=LH88 (in N59) | 100T | 11.47 | -0.95 | -0.18 | -1.42 | 1.93 | 0 | NA |
| SL598 | 40T | 13.46 | 0.18 | 0.61 | -1.28 | -0.08 | IVB | C |
| SL599 | 40T | 13.17 | -0.25 | 0.04 | -1.26 | -0.36 | II | C |
| LH86nw | 150T | 10.74 | -0.75 | 0.02 | -1.41 | 2.04 | 0 | A |
| NGC2041=SL605 | 60V | 10.36 | -0.17 | 0.22 | -1.48 | 2.51 | II | C |
| NGC2042=LH89n | 150T | 9.58 | -0.44 | 0.24 | -1.35 | 0.59 | I | A |
| LH89s | 150T | 10.80 | -0.77 | 0.08 | -1.33 | 0.55 | 0 | NA |
| SL601=BRHT16a=KMHK1130 (in NGC2042=LH89n) | 34T | 11.81 | -0.77 | 0.18 | -1.36 | 0.57 | I | C |
| NGC2044=SL602=LH90 (in N157=DEM263) | 150T | 10.59 | -0.73 | 0.10 | -1.32 | 0.31 | I | NA |
| LT- α =KMK88-79 (in NGC2044=SL602=LH90,in N157) | 40T | 11.93 | -0.52 | 0.60 | -1.31 | 0.30 | I | NC |
| SL607 | 50T | 12.63 | 0.15 | 0.55 | -1.40 | 0.69 | IVB | C |
| LT- ϵ (in NGC2044=SL602=LH90,in N157) | 50T | 12.82 | -0.68 | 0.14 | -1.31 | 0.31 | I | NC |
| LT- ζ =KMK88-87 (in NGC2044=SL602=LH90,in N157) | 34T | 11.23 | -0.65 | 0.35 | -1.33 | 0.33 | I | NC |
| HDE269828=LT- β =BRHT17b=KMK88-83 (in NGC2044,in N157) | 34T | 11.02 | -0.82 | 0.05 | -1.33 | 0.30 | 0 | NC |
| LH91 (in DEM251) | 150T | 11.01 | -0.75 | 0.24 | -1.54 | 3.06 | I | AN |
| LT- δ =BRHT17a=KMK88-88 (in NGC2044,in N157) | 34T | 11.37 | -0.54 | 0.24 | -1.35 | 0.30 | I | CN |
| LH92 (in DEM250) | 100T | 11.86 | -0.74 | 0.13 | -1.47 | 2.06 | I | NA |
| NGC2046=SL597 | 40T | 12.64 | -0.07 | 0.31 | -1.25 | -0.75 | III | C |
| NGC2047=SL600 | 40T | 13.15 | -0.24 | 0.23 | -1.28 | -0.70 | II | C |
| LH87s (in N154) | 150T | 10.48 | -0.79 | 0.07 | -1.29 | -0.18 | 0 | AN |
| NGC2048=N154A (in LH87n,in N154) | 50T | 12.17 | -0.99 | -0.12 | -1.31 | -0.15 | 0 | NA |
| NGC2050=SL609=LH93 (in LH96) | 150T | 9.25 | -0.78 | 0.22 | -1.38 | 0.11 | I | AN |
| NGC2051=SL608 | 50T | 11.69 | -0.06 | 0.34 | -1.26 | -1.52 | III | C |
| NGC2053=SL623 | 100T | 12.18 | -0.17 | 0.20 | -1.58 | 2.08 | II | C |
| NGC2055=SL610=LH94 (in LH96) | 150T | 8.39 | -0.55 | 0.12 | -1.38 | 0.00 | I | A |
| LH95 (in N64B=DEM252,in N61) | 150T | 11.10 | -0.95 | -0.09 | -1.57 | 3.16 | 0 | NA |
| HS367 (in LH95,in N64B=DEM252,in N61) | 40T | 13.42 | -0.84 | -0.05 | -1.57 | 3.13 | 0 | NC |
| LH96P1 (in LH96) | 150T | 10.67 | -0.85 | -0.13 | -1.38 | 0.05 | 0 | A |
| LH96P2 (in DEM261, in LH96) | 150T | 10.58 | -0.66 | 0.09 | -1.44 | 0.08 | I | NA |
| LH96P3 (in DEM261, in LH96) | 150T | 10.39 | -0.68 | 0.14 | -1.52 | 0.13 | I | NA |
| NGC2056=SL611 | 150T | 11.77 | -0.12 | 0.03 | -1.31 | -1.17 | III | C |
| NGC2057=SL616 | 40T | 12.17 | -0.13 | 0.22 | -1.36 | -0.77 | III | C |
| NGC2058=SL614 | 60V | 11.85 | -0.12 | 0.24 | -1.36 | -0.67 | III | C |
| NGC2059=SL613 | 40T | 12.85 | -0.09 | 0.31 | -1.37 | -0.63 | III | C |
| NGC2060=N157B=LH99 (in N157) | 150T | 9.59 | -0.66 | 0.10 | -1.50 | 0.33 | 0 | NA |
| NGC2065=SL626 | 60V | 11.24 | -0.10 | 0.26 | -1.42 | -0.74 | III | C |
| NGC2062=SL640 | 100T | 12.67 | -0.18 | 0.30 | -1.84 | 2.63 | II | C |
| NGC2066=SL627 | 40T | 13.10 | -0.08 | 0.35 | -1.43 | -0.67 | III | C |
| SL617 | 50T | 13.11 | 0.28 | 0.50 | -1.30 | -1.65 | IVB | C |
| LH97 (in DEM261,in LH96) | 150T | 9.97 | -0.72 | 0.14 | -1.45 | 0.18 | I | AN |
| HS370=LH98 (in LH96) | 100T | 10.38 | -0.60 | 0.05 | -1.45 | 0.06 | I | A |
| SL620=LW255 | 100TC | 12.62 | 0.20 | 0.69 | -1.11 | -4.91 | V | C |
| HS371=BRHT54a (sup ? LH97) | 34T | 12.97 | -0.05 | 0.28 | -1.46 | 0.16 | III | C |
| SL624 | 50T | 12.56 | -0.04 | 0.27 | -1.35 | -1.62 | III | C |
| SL628 | 100T | 12.32 | 0.02 | 0.49 | -1.66 | 2.17 | IVA | C |
| SL636 | 40T | 13.54 | 0.11 | 0.31 | -1.51 | -0.48 | IVA | C |
| SL639=M-OB3 (in N157) | 61CT | 11.37 | -0.28 | 0.60 | -1.64 | 0.31 | I | NC |
| M-OB1=H88-301 (sup ? in ? NGC2070=N157A=LH100) | 40T | 10.82 | -0.35 | 0.27 | -1.55 | 0.44 | I | CN |
| NGC2069 (in NGC2070=N157A=LH100,in N157) | 150T | 10.10 | -0.65 | -0.12 | -1.59 | 0.53 | 0 | NA |
| SL650 | 100T | 13.18 | -0.09 | 0.20 | -1.92 | 2.18 | III | C |
| 3DOR=SL633 (in NGC2070=N157A=LH100,in N157) | 187T | 7.25 | -0.56 | -0.02 | -1.57 | 0.41 | 0 | NC |
| NGC2072=SL630 | 40T | 13.21 | 0.04 | 0.52 | -1.49 | -0.74 | IVA | C |
| NGC2074=N158C=SL637=LH101 (in N158) | 150T | 9.32 | -0.91 | -0.16 | -1.59 | 0.00 | 0 | NA |
| NGC2075=N213 (in DEM265) | 100T | 11.47 | -0.77 | 0.01 | -1.46 | -1.19 | 0 | NA |
| NGC2077=N160D (in LH103,in N160,in LH106) | 50T | 11.71 | -0.71 | 0.00 | -1.62 | -0.16 | 0 | NC |
| NGC2078=N159F (in N159=SL644=LH105,in LH106) | 100T | 10.89 | -0.78 | 0.12 | -1.62 | -0.24 | 0 | NC |
| SL651 (sup DEM268) | 61C | 13.26 | 0.21 | 0.69 | -1.85 | 1.40 | V | C |
| NGC2079=N159A (in N159=SL644=LH105,in LH106) | 50T | 11.81 | -0.59 | -0.12 | -1.62 | -0.27 | 0 | NC |
| NGC2080=N160A=SL641 (in LH103,in N160,in LH106) | 50T | 10.42 | -0.61 | -0.04 | -1.64 | -0.15 | 0 | NC |
| LH103P1 (in N160=DEM284,in LH106) | 150T | 10.57 | -0.78 | 0.14 | -1.68 | -0.12 | 0 | NA |
| SL654 (sup DEM282) | 40T | 12.85 | -0.13 | 0.23 | -1.74 | -0.40 | III | C |
| IC2146=SL632=LW258 | 100T | 12.41 | 0.19 | 0.69 | -1.18 | -5.29 | V | C |

TABLE 1—Continued

| NAME | D(°) | V | U-B | B-V | X(°) | Y(°) | SWB | TYPE |
|--|-------|-------|-------|-------|-------|-------|-----|------|
| LH104 (in NGC2081,in N158) | 150T | 9.94 | -0.71 | 0.09 | -1.67 | 0.10 | I | AN |
| NGC2083=N159D (in N159=SL644=LH105,in LH106) | 100T | 10.83 | -0.96 | -0.11 | -1.65 | -0.24 | 0 | NC |
| NGC2084=N159C (in N159=SL644=LH105,in LH106) | 100T | 11.35 | -0.80 | 0.07 | -1.64 | -0.26 | 0 | NC |
| NGC2084e=N159C (in N159=SL644=LH105,in LH106) | 100T | 11.38 | -0.75 | -0.04 | -1.67 | -0.26 | 0 | NA |
| NGC2085=N160B (in LH103,in N160,in LH106) | 34T | 12.06 | -0.76 | -0.03 | -1.67 | -0.17 | 0 | NC |
| NGC2086=IC2145=N160C (in LH103,in N160,in LH106) | 50T | 12.00 | -0.72 | -0.08 | -1.69 | -0.17 | 0 | NC |
| IC2148=SL642=LW265 | 38C | 14.23 | 0.38 | 0.75 | -1.22 | -6.06 | VI | C |
| HS385=M-OB5 (in N160=DEM284,in LH106) | 34T | 12.33 | -0.63 | 0.23 | -1.72 | -0.04 | I | C |
| HS=SL648=LW268 | 38C | 13.30 | 0.33 | 0.77 | -1.51 | -2.69 | VI | C |
| M-OB4=H88-308 | 40T | 11.69 | -0.53 | 0.35 | -1.73 | 0.11 | I | C |
| NGC2088=SL652 (in DEM268) | 40T | 12.47 | -0.26 | 0.29 | -1.83 | 1.04 | I | C |
| NGC2091=SL653 (in LH106) | 40T | 12.03 | -0.61 | 0.38 | -1.76 | 0.07 | I | C |
| NGC2092 (in LH111,in DEM310) | 38CT | 12.17 | -0.49 | 0.57 | -1.81 | 0.28 | I | C |
| NGC2093=SL657=LH109 | 100T | 11.57 | -0.50 | 0.32 | -1.87 | 0.58 | I | CA |
| KMHK1251 | 40T | 12.80 | -0.67 | -0.05 | -1.94 | 1.14 | 0 | C |
| NGC2095=SL669 (in LH112) | 50T | 13.09 | -0.42 | 0.05 | -2.08 | 2.18 | I | C |
| NGC2096=SL664 | 40T | 11.36 | -0.17 | 0.49 | -1.95 | 1.05 | I | C |
| LH114 (in N70=DEM301) | 150T | 11.32 | -1.02 | -0.23 | -2.05 | 1.64 | 0 | NA |
| H6=SL668=LW274 | 100TC | 12.09 | 0.23 | 0.77 | -1.72 | -2.09 | VI | C |
| HS397A (in N164=LH113=DEM298,in DEM310) | 100T | 11.05 | -0.84 | -0.04 | -1.94 | 0.44 | 0 | NA |
| NGC2097=SL682=LW282 | 61C | 13.67 | 0.09 | 0.38 | -2.58 | 6.72 | IVA | C |
| NGC2098=SL667 | 78V | 10.73 | -0.58 | 0.16 | -1.98 | 1.23 | I | C |
| NGC2100=SL662 (in LH111,in DEM310) | 60V | 9.80 | -0.56 | 0.16 | -1.88 | 0.29 | I | C |
| NGC2102=SL665 (in DEM310) | 40T | 11.44 | -0.75 | -0.04 | -1.87 | 0.02 | 0 | C |
| NGC2103=N214C=SL660=LH110=DEM293 (in N214=LH107) | 150T | 10.82 | -0.87 | -0.24 | -1.69 | -1.83 | 0 | NA |
| SL674=ESO86SC26 | 61C | 13.33 | 0.05 | 0.67 | -2.21 | 3.24 | VII | C |
| SL675 | 100T | 12.01 | -0.39 | 0.22 | -2.10 | 1.92 | I | C |
| NGC2105=SL687 | 100T | 12.19 | -0.16 | 0.12 | -2.26 | 2.59 | III | C |
| N72=DEM302 (in LH115,in DEM306) | 100T | 12.98 | -1.06 | -0.05 | -2.24 | 3.24 | 0 | NC |
| SL676 | 100T | 13.03 | 0.38 | 0.67 | -1.86 | -1.07 | V | C |
| NGC2107=SL679 | 60V | 11.51 | 0.13 | 0.38 | -1.86 | -1.13 | IVA | C |
| SL678 | 38C | 14.30 | 0.13 | 0.60 | -2.24 | 3.30 | IVB | C |
| SL683 (in ? DEM310) | 100T | 12.61 | -0.23 | 0.42 | -1.98 | -0.28 | I | C |
| N71=DEM303 | 50T | 13.81 | -1.13 | -0.12 | -2.17 | 2.08 | 0 | NC |
| SL690 | 50T | 12.42 | -0.36 | 0.09 | -2.24 | 1.73 | I | C |
| NGC2108=SL686 | 62V | 12.32 | 0.22 | 0.58 | -2.04 | 0.33 | IVB | C |
| NGC2109=SL688 | 50T | 12.21 | -0.08 | 0.34 | -2.13 | 0.96 | III | C |
| NGC2111=SL699 | 50T | 12.45 | -0.07 | 0.30 | -1.94 | -1.49 | III | C |
| SL693 | 50T | 12.97 | -0.49 | 0.02 | -2.26 | 1.80 | I | C |
| SL695 | 50T | 12.91 | -0.42 | 0.25 | -2.25 | 1.68 | I | C |
| NGC2113 (in DEM311,in N168) | 100T | 12.33 | -0.92 | -0.14 | -2.12 | -0.27 | 0 | NA |
| NGC2117=SL718 | 100T | 11.65 | -0.14 | 0.36 | -2.55 | 2.06 | III | C |
| NGC2116=SL715 | 100T | 12.92 | -0.24 | 0.24 | -2.40 | 1.00 | II | C |
| NGC2114=SL706 | 100T | 12.48 | -0.67 | 0.08 | -2.34 | 1.46 | I | C |
| NGC2118=SL717 | 72V | 12.00 | -0.20 | 0.24 | -2.38 | 0.38 | II | C |
| SL710=LW298 | 61C | 13.57 | 0.04 | 0.18 | -2.79 | 5.63 | III | C |
| SL709 | 100T | 11.47 | -0.18 | 0.22 | -2.39 | 1.94 | II | C |
| SL723=LW302 | 38C | 13.60 | 0.20 | 0.71 | -1.99 | -3.66 | V | C |
| SL732 | 38C | 14.27 | 0.01 | 0.36 | -2.70 | 1.87 | IVA | C |
| SL734 | 38C | 12.45 | -0.02 | 0.28 | -2.29 | -1.55 | III | C |
| H7=SL735 | 100T | 12.26 | 0.02 | 0.60 | -2.74 | 1.79 | VII | C |
| NGC2120=SL742=LW316 | 61C | 12.67 | 0.21 | 0.64 | -3.21 | 5.84 | V | C |
| SL740 | 40T | 13.54 | 0.24 | 0.54 | -2.45 | -0.70 | IVB | C |
| SL746 | 50T | 13.33 | -0.38 | 0.15 | -2.82 | 1.93 | I | C |
| SL747 | 61C | 13.02 | 0.06 | 0.48 | -2.38 | -1.65 | IVA | C |
| NGC2121=SL725=LW303 | 62V | 12.37 | 0.25 | 0.84 | -2.19 | -1.97 | VI | C |
| SL748 | 100T | 12.66 | -0.04 | 0.25 | -2.47 | -0.91 | III | C |
| SL741=HS426 | 100T | 13.26 | 0.06 | 0.48 | -2.86 | 2.65 | IVA | C |
| NGC2122=N180B=SL731=LH117=DEM323 (in N180) | 150T | 10.43 | -0.90 | -0.12 | -2.39 | -0.56 | 0 | NA |
| SL749=LW317 | 38C | 14.12 | 0.12 | 0.41 | -2.17 | -3.53 | IVA | C |
| NGC2123=SL755=LW324 | 38C | 12.56 | -0.16 | 0.22 | -3.16 | 4.19 | III | C |
| NGC2127=SL751 | 50T | 11.64 | -0.14 | 0.33 | -2.68 | 0.15 | III | C |
| NGC2130=SL758 | 100T | 12.10 | -0.17 | 0.32 | -3.00 | 2.18 | II | C |
| NGC2133=SL757 | 50T | 12.40 | 0.03 | 0.35 | -2.49 | -1.66 | IVA | C |
| NGC2134=SL760 | 60V | 11.05 | -0.02 | 0.26 | -2.54 | -1.58 | III | C |
| SL753=LW325 | 100T | 13.53 | -0.01 | 0.42 | -3.11 | 3.64 | IVA | C |
| SL756 | 100T | 13.45 | 0.27 | 0.45 | -2.57 | -0.94 | IVB | C |
| NGC2135=SL765 | 100T | 12.05 | -0.22 | 0.17 | -3.11 | 2.09 | II | C |
| SL763 | 38C | 12.85 | -0.25 | 0.10 | -2.77 | -0.27 | II | C |
| NGC2136=SL762 | 60V | 10.54 | -0.13 | 0.28 | -2.81 | 0.02 | III | C |
| NGC2137=SL764 | 50T | 12.66 | -0.23 | 0.22 | -2.83 | 0.04 | II | C |
| NGC2145=SL780 | 100T | 12.07 | 0.05 | 0.37 | -2.76 | -1.38 | IVA | C |
| NGC2138=SL777=LW330 | 100T | 13.76 | -0.04 | 0.28 | -3.42 | 3.68 | III | C |
| SL769 | 61C | 13.18 | 0.01 | 0.68 | -2.77 | -0.55 | VII | C |
| SL774 | 100T | 13.46 | 0.31 | 0.42 | -2.98 | 0.50 | IVB | C |
| NGC2140=SL773 | 100T | 12.44 | -0.19 | 0.21 | -3.03 | 0.92 | II | C |
| H8=SL771 | 77C | 12.77 | 0.15 | 0.62 | -3.11 | 1.78 | IVB | C |
| SL776=LW328 | 38C | 14.17 | 0.38 | 0.82 | -2.43 | -3.54 | VI | C |
| SL783=LW333 | 61C | 13.85 | 0.23 | 0.69 | -2.31 | -5.09 | V | C |
| NGC2147=SL784 (in N75B=LH122) | 50T | 12.94 | -0.36 | 0.26 | -3.22 | 1.32 | I | CN |
| SL785 (in N75B=LH122) | 100T | 11.83 | -0.97 | -0.19 | -3.20 | 1.33 | 0 | NA |
| SL791 | 100T | 13.45 | -0.17 | 0.02 | -3.27 | 0.91 | III | C |
| SL788=LW336 | 100T | 13.28 | 0.32 | 0.68 | -2.83 | -1.67 | V | C |

TABLE 1—Continued

| NAME | D(”) | V | U-B | B-V | X(°) | Y(°) | SWB | TYPE |
|---------------------|-------|-------|-------|------|-------|-------|-----|------|
| NGC2153=SL792=LW341 | 100T | 13.05 | 0.03 | 0.69 | -3.66 | 3.12 | VII | C |
| H9=SL790 | 77C | 12.67 | 0.12 | 0.58 | -2.97 | -0.82 | IVB | C |
| NGC2154=SL793=LW339 | 150T | 11.79 | 0.25 | 0.68 | -3.52 | 2.26 | V | C |
| NGC2155=SL803=LW347 | 62V | 12.60 | 0.23 | 0.81 | -3.85 | 4.05 | VI | C |
| NGC2156=SL796 | 72V | 11.38 | -0.07 | 0.12 | -3.37 | 1.06 | III | C |
| NGC2157=SL794 | 60V | 10.16 | -0.16 | 0.19 | -3.25 | 0.33 | III | C |
| NGC2159=SL799 | 72V | 11.38 | -0.14 | 0.28 | -3.37 | 0.90 | III | C |
| NGC2160=SL801 | 100T | 12.16 | -0.14 | 0.20 | -3.43 | 1.23 | III | C |
| NGC2161=SL789=LW337 | 61C | 12.95 | 0.25 | 0.80 | -2.41 | -4.83 | VI | C |
| H10=SL800=LW349 | 38C | 13.79 | 0.24 | 0.80 | -3.61 | 2.42 | VI | C |
| SL804=LW346 | 61C | 13.82 | 0.27 | 0.66 | -2.57 | -4.65 | V | C |
| IC2161=SL802=LW345 | 38C | 14.24 | 0.13 | 0.66 | -2.42 | -5.62 | V | C |
| NGC2162=SL814=LW351 | 62V | 12.70 | 0.31 | 0.68 | -4.30 | 5.80 | V | C |
| NGC2164=SL808 | 60V | 10.34 | -0.24 | 0.10 | -3.47 | 1.01 | II | C |
| NGC2172=SL812 | 72V | 11.75 | -0.16 | 0.18 | -3.56 | 0.89 | III | C |
| NGC2166=SL811 | 50T | 12.86 | 0.09 | 0.26 | -3.61 | 1.58 | IVA | C |
| NGC2173=SL807=LW348 | 150TC | 11.88 | 0.28 | 0.82 | -2.76 | -3.46 | VI | C |
| SL817 | 38C | 14.18 | 0.16 | 0.72 | -3.40 | -0.54 | VII | C |
| NGC2177=SL816=LW355 | 61C | 12.83 | -0.32 | 0.14 | -3.80 | 1.79 | II | C |
| NGC2181=SL825=LW366 | 38C | 13.64 | 0.07 | 0.29 | -4.32 | 4.26 | IVA | C |
| ESO121SC03=KMHK1591 | 61C | 14.04 | 0.17 | 0.87 | -4.94 | 9.00 | VII | C |
| SL823=SL820=LW362 | 61C | 13.59 | 0.16 | 0.62 | -4.41 | 5.20 | IVB | C |
| NGC2190=SL819=LW357 | 61C | 12.94 | 0.29 | 0.63 | -2.72 | -5.20 | V | C |
| SL828=LW367 | 61C | 13.65 | 0.20 | 0.51 | -2.88 | -4.66 | IVB | C |
| NGC2193=SL839=LW387 | 38C | 13.42 | 0.20 | 0.71 | -4.72 | 4.43 | V | C |
| NGC2197=SL838=LW385 | 38C | 13.45 | 0.12 | 0.37 | -4.37 | 2.44 | IVA | C |
| NGC2203=SL836=LW380 | 150T | 11.29 | 0.26 | 0.77 | -2.84 | -5.91 | VI | C |
| SL842=LW399 | 38C | 14.15 | 0.11 | 0.79 | -5.29 | 6.55 | VII | C |
| NGC2209=SL849=LW408 | 68V | 13.15 | 0.20 | 0.53 | -3.38 | -4.30 | IVB | C |
| NGC2210=SL858=LW423 | 68V | 10.94 | 0.12 | 0.70 | -4.51 | 0.42 | VII | C |
| NGC2213=SL857=LW419 | 62V | 12.38 | 0.28 | 0.71 | -3.98 | -1.99 | V | C |
| NGC2214=SL860=LW426 | 60V | 10.93 | -0.27 | 0.11 | -4.80 | 1.28 | II | C |
| SL862=LW431 | 38C | 13.67 | 0.13 | 0.74 | -4.36 | -1.16 | VII | C |
| SL866=LW438 | 24C | 13.65 | 0.23 | 0.71 | -5.41 | 3.56 | V | C |
| H11=SL868=LW437 | 61C | 11.93 | 0.01 | 0.64 | -4.61 | -0.31 | VII | C |
| SL870=LW440 | 38C | 13.43 | 0.19 | 0.69 | -4.05 | -3.07 | V | C |
| SL873=LW447 | 100T | 13.77 | -0.03 | 0.41 | -4.93 | 0.41 | IVA | C |
| SL874=LW446 | 38C | 13.06 | 0.22 | 0.78 | -4.70 | -0.53 | VI | C |
| NGC2231=SL884=LW466 | 44V | 13.20 | 0.24 | 0.67 | -5.70 | 2.03 | V | C |
| NGC2241=SL888=LW471 | 38C | 13.25 | 0.23 | 0.77 | -5.57 | 0.63 | VI | C |
| NGC2249=SL893=LW479 | 150T | 11.94 | 0.20 | 0.42 | -5.84 | 0.64 | IVB | C |
| NGC2257=SL895=LW481 | 61C | 12.62 | 0.01 | 0.62 | -7.44 | 5.23 | VII | C |
| SL897=LW483 | 38C | 14.04 | 0.24 | 0.56 | -5.86 | -1.56 | IVB | C |

NOTES.—All coordinates below are for J1950.0. Previously anonymous objects are denoted by BCDS 1, $\alpha = 4^{\text{h}}56^{\text{m}}13^{\text{s}}$, $\delta = -66^{\circ}31'55''$ (small association in the large complex LH 9); BCDS 2, $\alpha = 5^{\text{h}}22^{\text{m}}28^{\text{s}}$, $\delta = -67^{\circ}59'21''$ (association embedded in an emission ring that is the western part of DEM 152); BCDS 3, $\alpha = 5^{\text{h}}25^{\text{m}}08^{\text{s}}$, $\delta = -66^{\circ}41'20''$ (association that includes the cluster SL 452); BCDS 4, $\alpha = 5^{\text{h}}28^{\text{m}}30^{\text{s}}$, $\delta = -67^{\circ}40'40''$ (association that has the cluster SL 497 = KMHK 940 in its center); BCDS 5, $\alpha = 5^{\text{h}}31^{\text{m}}54^{\text{s}}$, $\delta = -66^{\circ}09'50''$ (association that includes the cluster pair SL 550 = BRHT 37a = KMHK 1017 and BRHT 37b = KMHK 1020); BCDS 6, $\alpha = 5^{\text{h}}32^{\text{m}}22^{\text{s}}$, $\delta = -67^{\circ}42'46''$ (small cluster in NGC 2014); BCDS 7, $\alpha = 5^{\text{h}}31^{\text{m}}56^{\text{s}}$, $\delta = -68^{\circ}35'19''$ (compact cluster $\sim 1'$ south of SL 552); BCDS 8, $\alpha = 5^{\text{h}}35^{\text{m}}10^{\text{s}}$, $\delta = -69^{\circ}46'36''$ (compact cluster in the association NGC 2033). The UBV values for the following clusters were corrected for bright, superimposed stars; the diaphragms and the values for the stars are as follows: SL 133, $D = 19^{\text{h}}C$, $V = 12.99$ mag, $(U - B) = 0.66$ mag, $(B - V) = 0.06$ mag; NGC 1786, $D = 15^{\text{h}}V$, $V = 10.95$ mag, $(U - B) = 0.00$ mag, $(B - V) = 0.61$ mag; SL 410, $D = 19^{\text{h}}C$, $V = 10.89$ mag, $(U - B) = 0.02$ mag, $(B - V) = 0.33$ mag; NGC 1942, $D = 19^{\text{h}}C$, $V = 13.65$ mag, $(U - B) = 0.71$ mag, $(B - V) = 0.95$ mag; NGC 1997, $D = 19^{\text{h}}C$, $V = 13.87$ mag, $(U - B) = 0.09$ mag, $(B - V) = 0.58$ mag; SL 576, $D = 19^{\text{h}}C$, $V = 11.99$ mag, $(U - B) = 1.04$ mag, $(B - V) = 1.51$ mag; NGC 2097, $D = 19^{\text{h}}C$, $V = 13.90$ mag, $(U - B) = 0.30$ mag, $(B - V) = 0.71$ mag; SL 710, $D = 19^{\text{h}}C$, $V = 11.81$ mag, $(U - B) = 0.04$ mag, $(B - V) = 0.58$ mag. The following objects have often been misidentified in the literature; our observations refer to the objects at the indicated coordinates: NGC 1745, $\alpha = 4^{\text{h}}54^{\text{m}}32^{\text{s}}$, $\delta = -69^{\circ}14'11''$ ($\sim 1.2'$ north of NGC 1748); NGC 1934, $\alpha = 5^{\text{h}}21^{\text{m}}58^{\text{s}}$, $\delta = -67^{\circ}57'10''$ ($\sim 1.1'$ east and $0.3'$ north of NGC 1929). The following objects are considerably more extended than the employed diaphragm; the observed region corresponds to the coordinates: NGC 1845, $\alpha = 5^{\text{h}}06^{\text{m}}23^{\text{s}}$, $\delta = -70^{\circ}35'40''$; NGC 1925n, $\alpha = 5^{\text{h}}21^{\text{m}}42^{\text{s}}$, $\delta = -65^{\circ}48'30''$; NGC 1925s, $\alpha = 5^{\text{h}}21^{\text{m}}55^{\text{s}}$, $\delta = -65^{\circ}53'00''$ (diaphragm includes SL 415); SL 417P1, part of SL 417, $\alpha = 5^{\text{h}}22^{\text{m}}05^{\text{s}}$, $\delta = -67^{\circ}58'50''$ (diaphragm excludes NGC 1929, 1934, 1935, 1936); LH 77P1, $\alpha = 5^{\text{h}}34^{\text{m}}12^{\text{s}}$, $\delta = -67^{\circ}00'45''$, LH 77P2, $\alpha = 4^{\text{h}}56^{\text{m}}13^{\text{s}}$, $\delta = -66^{\circ}31'55''$, and LH 77P3, $\alpha = 5^{\text{h}}31^{\text{m}}25^{\text{s}}$, $\delta = -67^{\circ}03'40''$ (parts of the large association or star cloud LH 77); LH 69P1, $\alpha = 5^{\text{h}}31^{\text{m}}20^{\text{s}}$, $\delta = -71^{\circ}05'41''$ (diaphragm excludes NGC 2018); NGC 2034n, $\alpha = 5^{\text{h}}35^{\text{m}}37^{\text{s}}$, $\delta = -66^{\circ}54'00''$; NGC 2034s, $\alpha = 5^{\text{h}}35^{\text{m}}43^{\text{s}}$, $\delta = -66^{\circ}57'10''$; LH 87s, $\alpha = 5^{\text{h}}35^{\text{m}}57^{\text{s}}$, $\delta = -69^{\circ}43'39''$; LH 86nw, $\alpha = 5^{\text{h}}36^{\text{m}}03^{\text{s}}$, $\delta = -67^{\circ}29'17''$; LH 89s, $\alpha = 5^{\text{h}}36^{\text{m}}11^{\text{s}}$, $\delta = -69^{\circ}00'30''$; LH 96P1, $\alpha = 5^{\text{h}}37^{\text{m}}12^{\text{s}}$, $\delta = -69^{\circ}28'41''$, LH 69P2, $\alpha = 5^{\text{h}}37^{\text{m}}12^{\text{s}}$, $\delta = -69^{\circ}28'41''$, and LH 96P3, $\alpha = 5^{\text{h}}38^{\text{m}}31^{\text{s}}$, $\delta = -69^{\circ}23'21''$ (parts of the large association or star cloud LH 96; LH 96P1 and LH 96P2 are embedded in DEM 261, which occupies the eastern part of LH 96); LH 103P1, $\alpha = 5^{\text{h}}40^{\text{m}}45^{\text{s}}$, $\delta = -69^{\circ}37'45''$ (diaphragm excludes NGC 2077, 2080, 2085, 2086). The diaphragms for the following objects include or exclude other objects as indicated: KMHK 341 includes N91B and IC 2117 = N91A; NGC 1777 excludes the two bright foreground stars; NGC 1820 excludes NGC 1816; LH 23 includes SL 209; SL 320 includes NGC 1874 = N113D, NGC 1876 = N113C, and NGC 1877 = N113A + B + E; NGC 1918 includes N120A, B, and C; NGC 1968e includes N51C; N44K includes N44G; SL 456 includes N51B; ESO 86SC2 = KMHK 981 is an association that includes the cluster SL 521 = LW 227; SL 553s ($\alpha = 5^{\text{h}}32^{\text{m}}21^{\text{s}}$, $\delta = -66^{\circ}30'10''$) includes N55A; SL 553n ($\alpha = 5^{\text{h}}32^{\text{m}}06^{\text{s}}$, $\delta = -66^{\circ}27'33''$) includes DEM 228a; NGC 2015 is an association that includes the cluster pair SL 557 = BRHT 15a and BRHT 15b; LH 70 excludes HS 341; N148C = LH 71 includes BCDS 7 and SL 552 = KMHK 1024; NGC 2113 includes N168A and N168B; LH 114 includes SL 673; NGC 2075 includes N213A = SL 631; NGC 2044 includes the clusters HDE 269828 = LT- β , LT- γ , and LT- δ ; NGC 2042 includes the cluster pair SL 601 = BRHT 16a = KMHK 1130 and BRHT 16b = KMHK 1131; NGC 2030 includes the SNR N63A; LH 95 includes HS 367; LH 97 includes the cluster KMK88-91 = H88-297 and excludes the pair HS 371 = BRHT 54a and BRHT 54b = H88-298. Other remarks: SL 178 is a cluster at $\alpha = 5^{\text{h}}01^{\text{m}}35^{\text{s}}$, $\delta = -65^{\circ}53'36''$ and has often been designated in the literature as NGC 1787, but the original NGC description fits the appearance of the association LH 15, where the cluster is embedded. BCD 1, at $\alpha = 5^{\text{h}}21^{\text{m}}54^{\text{s}}$, $\delta = -69^{\circ}28'50''$, is the anonymous cluster in Bica et al. 1992. N49 is a supernova remnant. The diaphragm for SL 485 = BRHT 36a = KMHK 923 includes its companion cluster BRHT 36b = KMHK 922, and both are embedded in a large, anonymous association. The original NGC description of NGC 1983 fits the appearance of the association LH 61, instead of the compact cluster SL 492 in its center. M-OB 1 = H88-301 is a small cluster embedded in the 30 Dor nebulosity; its UBV values are averages of the two sets in Table 2, which have background sky respectively outside the 30 Dor complex and adjacent to the cluster.

urn 1976). Other abbreviations refer to objects described in Heydari-Malayeri, Niemela, & Testor (1987; HNT), Lortet & Testor (1984; LT), Robertson (1974; Rob), Melnick (1987; M-OB), Bica, Clariá, & Dottori (1992; BCD), and this paper (BCDSP). Also included are some objects from catalogs of stars that are in fact compact clusters and/or emission nebulae. Column (1) contains the object cross-identifications in different catalogs and also provides in parentheses indications of larger objects at the same location (“sup” denotes a superimposition and “in” denotes inclusion).

We present in column (9) of Table 1 the classification of the 624 sample objects in terms of star cluster (C), very young cluster embedded in H II region or compact H II region (NC), stellar associations without gas (A), associations embedded in H II regions (NA), and star clusters and associations with traces of emission (CN and AN, respectively). Objects with intermediate properties were classified as CA or AC. In addition, we list the supernova remnant (SNR) N49 for comparison purposes.

Regarding the photometric data, Table 1 contains three types of results: (1) objects with complete UBV data taken from VDB81 and references therein that did not have any remarks on possible uncertainties; (2) objects from VDB81 that we re-observed in order to check uncertainties, and (3) new objects. Our observations were carried out at the Cerro Tololo Inter-American Observatory (CTIO), Chile, in 1989 December, 1990 November, and 1991 January and at the Complejo Astronómico El Leoncito (CASLEO), Argentina, in 1990 March and December. In Table 1 we present for each object a single V , $U - B$, and $B - V$ set (cols. [3]–[5]), corresponding to the largest diaphragm available (except in a few cases, in order to avoid contamination by atypical bright stars, rich fields, or companion objects). Each diaphragm diameter (in arcseconds) in column (2) is labeled V, T, or C to indicate the photometry source, respectively VDB81 or the present CTIO or CASLEO observations. These labels and the cluster identifications allow comparison of the photometry of individual objects in common with VDB81’s compilation. In BCD92 (the bar region) a detailed discussion of individual objects in common with VDB81 was presented, and a few discrepancies were detected, arising, for example, from differing diaphragm sizes and/or sampling (mainly for H II/OB complexes), possible misidentifications in previous works, and background effects. In the present global sample a few discrepancies were detected outside the bar region as well, where background effects are less important.

Table 1 contains $\sim 60\%$ objects with photometry published for the first time, $\sim 20\%$ from Bica et al. (1991) and BCD92, and $\sim 20\%$ from VDB81 and references therein. In Table 2 we present complementary observations, with additional diaphragms, not presented in Bica et al. (1991) or BCD92.

The procedures employed in the observations, the reduction method, and the error analysis of the CTIO data were discussed in detail in BCD92. We recall below main points of the CTIO observations and discuss in more detail the CASLEO ones. In both cases the background regions for the objects were previously selected on plates in order to avoid atypical bright stars.

2.1. CTIO Observations

The CTIO observations were carried out on the 61 cm Lowell telescope with a single-channel photometer equipped with a dry-ice-refrigerated EMI 9781A photomultiplier. The

U filter was blocked with a 2 mm solid crystal of CuSO_4 in order to suppress the red leak. Standard stars from Graham (1982) were observed, and extinction coefficients were computed nightly. In particular, the very hot standard HD 49798 was fundamental to the derivation of the colors of very young objects. The observations of the star clusters consisted of 30 s integrations for cluster and background regions that were repeated until 1% precision was attained. External and internal mean errors are nearly the same as those of BCD92 for bar clusters, which correspond to observations mostly from the first CTIO run. Here we simply recall that for 17 bar clusters repeated in different nights the agreement was better than 0.04 mag in all indices; for the new objects, the errors are smaller since crowding and background inhomogeneities are less important outside the bar.

2.2. CASLEO Observations

The CASLEO runs were dedicated mostly to the fainter clusters in the sample. The measurements were made with the Boller & Chivens 2.15 m telescope and the photoelectric photometer mode of the VATPOL photopolarimeter (Magalhães, Benedetti, & Roland 1984). The instrument is equipped with two Ga-As RCA 31034 photomultipliers refrigerated with dry ice. A UBV filter set, blocked with CuSO_4 , was used to eliminate the red leak. The nights were of good photometric quality, with a typical seeing of $\sim 2''$. In order to determine the extinction, a pair of blue and red stars was observed nightly through an air-mass range $1.3 < \text{AM} < 2.0$. These stars are numbers 1 and 2 in the Bok and Tifft sequence, as revised by Alcaíno & Liller (1982). The following mean first-order coefficients were obtained for the March run: $K_V = 0.20$, $K_{B-V} = 0.12$, and $K_{U-B} = 0.17$. In the December run, the values were 0.16, 0.10, and 0.20, respectively. The extinction coefficients determined in both periods thus appear to be close to the typical mean values for CASLEO (Minniti, Clariá, & Gomez 1989). The UBV standard stars are from Graham (1982), and the instrumental transformations proved to be systematically linear (to about 0.03 mag) over the full range in color of the standards [$0.01 \text{ mag} < (B - V) < 1.33 \text{ mag}$, $-0.43 \text{ mag} < (U - B) < 1.35 \text{ mag}$]. The reductions were made at the Córdoba observatory in the usual manner. A comparison of the observed mean values with the published ones for the standard stars yields the external mean errors of a single observation. Typical values were found to be $\sigma_V = 0.022$, $\sigma_{B-V} = 0.016$, and $\sigma_{U-B} = 0.019$, which indicates that the UBV system has been well reproduced.

The integrations for the star clusters were made essentially in the same way as those at CTIO (§ 2.1). The UBV internal errors analyzed as a function of the integrated V magnitude showed that the average internal errors in V and $B - V$ are respectively 0.01 and 0.02 mag, even for the fainter clusters in the sample ($14.0 \text{ mag} < V < 14.5 \text{ mag}$). The average internal errors in $U - B$ are 0.02 mag for clusters brighter than $V = 13.0$ mag, whereas for those of $V \sim 14.0$ mag or fainter we derived a value of 0.05 mag. This relatively larger internal error is due to the sensitivity decrease of the RCA 31034 phototube in the ultraviolet region.

3. ANALYSIS OF THE UBV PHOTOMETRY

We show in Figures 1a and 1b the V histograms, respectively, for the star clusters and the associations. We distinguish

TABLE 2
COMPLEMENTARY OBSERVATIONS

| NAME | D(") | V | U-B | B-V |
|---|------|-------|-------|-------|
| RETICULUM=Sersic40/3=ESO118SC31=KMHK10 | 77C | 14.72 | 0.26 | 0.53 |
| NGC1652=SL10=LW14 | 38C | 13.36 | 0.25 | 0.84 |
| NGC1714=N4A=SL64=DEM8b | 40T | 11.75 | -0.68 | -0.12 |
| SL92 | 50T | 13.51 | 0.14 | 0.62 |
| SL123 (in LH8=DEM36) | 34T | 12.58 | -0.58 | -0.10 |
| NGC1841=ESO4SC15 | 61C | 12.55 | 0.09 | 0.85 |
| NGC1841=ESO4SC15 | 187T | 11.43 | 0.21 | 0.75 |
| NGC1859=SL297=LW156 | 50T | 12.26 | -0.11 | 0.44 |
| NGC1882=SL340 | 50T | 13.00 | -0.21 | 0.01 |
| H2=SL363 | 40T | 12.32 | 0.25 | 0.57 |
| SL390 | 34T | 13.46 | -0.10 | 0.50 |
| SL463=LW213 (in LH53) | 50T | 12.41 | -0.28 | 0.14 |
| SL505 | 50T | 13.14 | 0.14 | 0.73 |
| SL551 | 40T | 13.43 | -0.20 | 0.13 |
| H3=SL569 | 40T | 13.42 | 0.40 | 0.94 |
| H3=SL569 | 38C | 13.52 | 0.55 | 0.89 |
| SL579 | 40T | 13.08 | -0.51 | 0.21 |
| SL585 | 40T | 12.84 | -0.13 | 0.40 |
| SL585 | 38C | 12.89 | -0.06 | 0.41 |
| SL620=LW255 | 100T | 12.62 | 0.24 | 0.66 |
| SL620=LW255 | 61C | 12.92 | 0.15 | 0.73 |
| SL639=M-OB3 (in N157) | 40T | 11.53 | -0.20 | 0.60 |
| SL639=M-OB3 (in N157) | 61C | 11.37 | -0.36 | 0.61 |
| M-OB1=H88-301 (sup? in? NGC2070=N157A=LH100) | 40T | 10.89 | -0.32 | 0.29 |
| M-OB1=H88-301 (sup? in? NGC2070=N157A=LH100) | 40T | 10.74 | -0.38 | 0.25 |
| 30 DOR=SL633 (in NGC2070=N157A=LH100,in N157) | 150T | 7.47 | -0.57 | 0.04 |
| 30 DOR=SL633 (in NGC2070=N157A=LH100,in N157) | 100T | 7.85 | -0.62 | 0.09 |
| 30 DOR=SL633 (in NGC2070=N157A=LH100,in N157) | 50T | 8.45 | -0.71 | 0.12 |
| NGC2091=SL653 (in LH106) | 38C | 12.07 | -0.59 | 0.32 |
| NGC2092 (in LH111,in DEM310) | 40T | 12.27 | -0.56 | 0.58 |
| NGC2092 (in LH111,in DEM310) | 38C | 12.17 | -0.42 | 0.56 |
| NGC2096=SL664 | 38C | 11.31 | -0.14 | 0.51 |
| H6=SL668=LW274 | 100T | 12.09 | 0.25 | 0.79 |
| H6=SL668=LW274 | 61C | 12.48 | 0.21 | 0.76 |
| SL676 | 40T | 13.16 | 0.42 | 0.57 |
| NGC2136=SL762 | 50T | 10.70 | -0.13 | 0.29 |
| NGC2173=SL807=LW348 | 150T | 11.88 | 0.25 | 0.86 |
| NGC2173=SL807=LW348 | 61C | 12.40 | 0.31 | 0.77 |
| NGC2203=SL836=LW380 | 61C | 11.98 | 0.39 | 0.82 |
| NGC2249=SL893=LW479 | 100T | 12.17 | 0.21 | 0.39 |

NOTE.—The background for the first observation of M-OB 1 was set outside the 30 Dor complex, whereas that for the second observation was adjacent to M-OB 1, which is embedded in the emission.

in each case the histograms corresponding to the total sample and the fraction associated with gas emission; among the associations, the fraction presenting gas emission is dominant. The trend of the histogram for the total sample of star clusters suggests that it is essentially complete up to $V \sim 13.0$ mag, but the number of observed fainter clusters is considerable. The interpretation of the behavior of the histogram for the associations is not as straightforward as that for the clusters because, in some cases, the associations are more extended than the largest available diaphragm. In any case, the total number of observed associations (120) is considerable in terms of cataloged ones; most of the Lucke & Hodge (1970) associations were observed.

We present in Figures 2a and 2b the observed $(U - B) \times (B - V)$ diagrams, respectively, for the star clusters (NC, CN, C, and CA) and the associations (NA, AN, A, and AC). The colors corrected for foreground reddening can be obtained with the normal reddening law ratio $E(U - B)/E(B - V) = 0.76$ and the foreground reddening in the direction of the LMC $E(B - V) = 0.06$ (Mould & Aaronson 1980). We indicate in Figures 2a and 2b a dereddening arrow of $E(B - V) = 0.20$, which is a typical internal reddening found in LMC H II regions, associations, and young star clusters (see, e.g., Lee 1991). The observed UBV color-color distribution can be related to the SWB classification (originally based on the Gunn photometric system), which is basically an age sequence, except for the SWB VII group, in which a metallicity effect is important

(see Chiosi, Bertelli, & Bressan 1988; Girardi & Bica 1993). Following the definitions in BCD92, we indicate in the present figures the UBV -equivalent SWB type zones. They include the SWB 0 type (for very young clusters, mostly embedded in gas emission), which BCD92 introduced together with the division of the SWB IV type (see discussion below).

The youngest H II regions in the LMC are not located at the upper-left corner of the color-color diagram, but around $(U - B) \sim -0.6$ mag and $(B - V) \sim -0.2$ mag. We illustrate this in Figures 2a and 2b by marking the loci of NGC 1714 (N4A), 30 Dor (NGC 2070), and NGC 2032, which are among the most excited objects in the LMC (Dufour & Harlow 1977; Dottori & Bica 1981). This effect is basically caused by the relative intensity of the emission lines and their distribution in the UBV filters. A detailed discussion of this effect with a large sample of spectra is given in Santos et al. (1995). As a consequence, the evolution of the H II region plus ionizing stars in the color-color diagram (Figs. 2a, 2b) follows a hook-shaped path in the SWB 0 zone.

The integrated colors of star clusters around 10 Myr may reach very red $B - V$ colors owing to the red supergiant phase (Arimoto & Bica 1989; Girardi & Bica 1993). The clusters in this phase that have been studied by means of near-infrared spectra in Bica, Alloin, & Santos (1990) are all located in the SWB I zone and are distinguished in Figure 1a. Other star clusters near these loci, as well as associations in Figure 2b, are

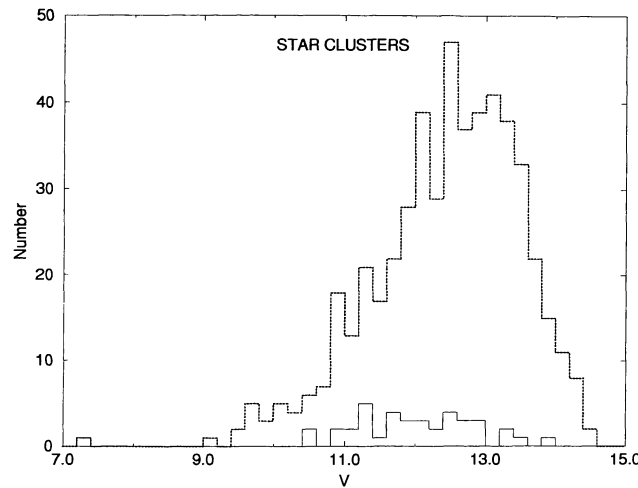


FIG. 1a

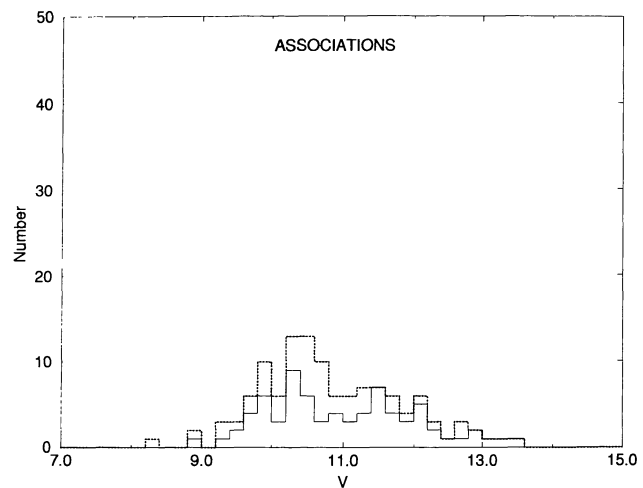


FIG. 1b

FIG. 1.— V magnitude histograms for (a) star clusters and (b) associations. Dashed lines represent the total sample and continuous lines the fraction corresponding to objects associated with emitting gas.

candidates to contain red supergiant stars. The extension of the distribution of points in the SWB I zone to colors as red as $(B - V) \sim 0.6$ mag is caused by stochastic effects of red supergiant stars in poorly populated clusters, as shown in the simulations by Girardi & Bica (1993).

The division of the SWB IV type into SWB IVA and SWB IVB corresponds to clusters respectively bluer and redder than a gap in the distribution of objects in the color-color diagram,

which is possibly related to the He flash and the first appearance of the red giant-branch stars (see Bica et al. 1991 and also the recent results of Corsi et al. 1994).

The star cluster Reticulum (Sérsic 40/3) is known to have an age comparable to those of Galactic globular clusters (Gratton & Ortolani 1987), and it contains RR Lyrae stars (Walker 1991). We attributed accordingly the SWB VII type to this cluster (Table 1), but its colors are those of an SWB V cluster,

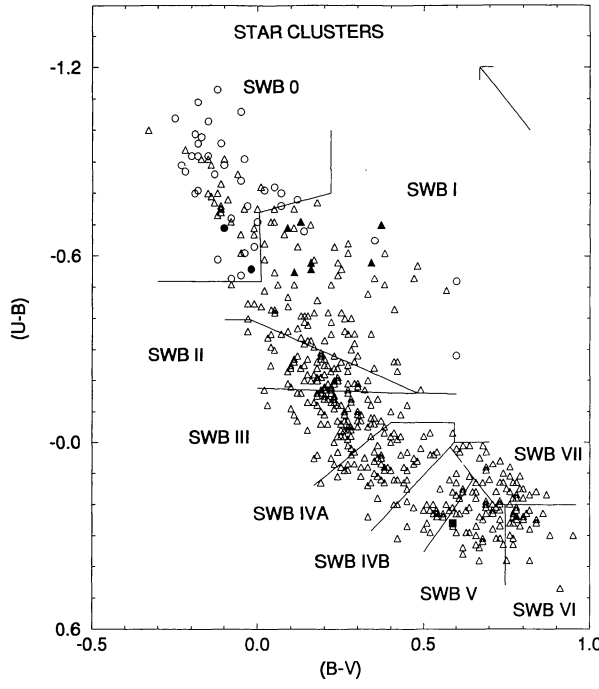


FIG. 2a

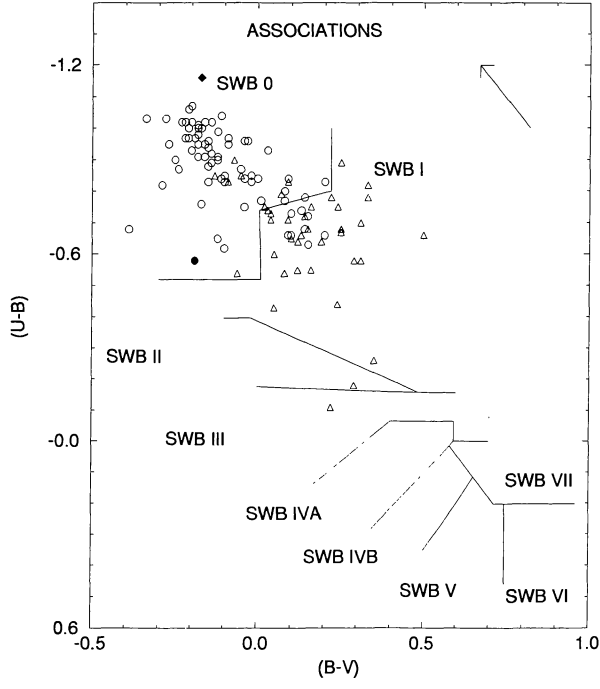


FIG. 2b

FIG. 2.—Color-color diagram for (a) star clusters and (b) associations. Triangles are objects without emitting gas, and circles are objects related to emitting gas. Filled circles are very excited H II regions. Filled triangles are clusters with red supergiants. The filled square is the cluster Reticulum. Filled diamond is the SNR N49. The borderlines of the SWB zones and a dereddening arrow for $E(B - V) = 0.20$ are shown.

as indicated in Figure 2a. The bright foreground star number 28 of Demers & Kunkel (1976) was not included in our observations in both the employed diaphragms (Tables 1 and 2). The exceedingly blue $B - V$ color for this metal-poor globular cluster is due to the very poorly populated giant branch, as can be seen in the H-R diagrams (Demers & Kunkel 1976; Gratton & Ortolani 1987). A counterpart of this effect among Galactic globular clusters is NGC 7492, which has observed integrated colors $(U - B) = 0.23$ mag and $(B - V) = 0.42$ mag and reddening $E(B - V) = 0.01$ (see Reed 1985 and references therein), which would place it in the SWB IVB region (taking into account the foreground reddening of the LMC). Table 1 and Figure 2a contain 37 clusters located in the SWB VII zone, most of them reported as such for the first time. These clusters are candidates for having ages comparable to those of Galactic globular clusters, and in order to check this possibility it would be necessary to obtain H-R diagrams and survey them for RR Lyrae stars. The only cluster known so far to be in the apparent age gap between 3 and 10 Gyr in the star-formation history of the LMC (Jensen, Mould, & Reid 1988) is ESO 121SC3 (Mattoo, Hodge, & Schommer 1986), which is located in the SWB VII zone (Table 1, Fig. 2a). Hence, another important reason for a detailed analysis of the new SWB VII sample is the possibility that other clusters in this age gap may be detected.

We indicate properties of the SWB groups in Table 3: the second column contains the age range according to the calibration in BCD92; the third, fourth, and fifth columns contain respectively the number of star clusters, associations, and their sum for each SWB type. The number of clusters in each age group is related to the formation and disruption rates of the stellar system and depend as well on the object mass and the observational luminosity cutoff. Girardi & Bica (1993) inferred the intrinsic age-distribution function based on the present global sample, taking into account how the cluster luminosity evolves (fading lines for model clusters).

The associations in the color-color diagram (Fig. 2b) are mainly distributed in the SWB 0–I zones. We distinguish in Figure 2b associations with and without emitting gas. In the SWB 0 zone, 87% of the associations have emission, while in the SWB I zone the figure is only 17%. In the case of star clusters, 51% of those in the SWB 0 zone have emitting gas,

whereas only 6% in the SWB I zone do. These fractions are related to the evolution of H II regions, combining the effects of the evolution of ionizing stars and the development of stellar winds. The differences in the fraction of objects having gas emission between star clusters and associations suggest that the mechanisms of gas sweeping are more efficient in the clusters.

Two associations (LH 7 and BCDS 4) are located in the SWB II–III zones (as old as 100 Myr, according to the age calibration of SWB types in BCD92, which is hereafter adopted). They have two properties in common: they are located at more than 2 kpc from the center of the bar (near the edge of the H II region disk, § 4) and have embedded star clusters (SL 111 and BRHT 25b in LH 7, SL 497 in BCDS 4), which may contribute to their dynamical stability so as to survive for such a long time. The numbers of associations in the groups SWB 0, SWB I, and SWB II+III are 77, 41, and 2, respectively, which is a result of the rates of formation and disruption of stellar associations. We also marked in Figure 2b the SNR N49, which is located in the SWB 0 zone, being the bluest object in $U - B$ in the entire object sample. Intrinsically, N49 very probably belongs to the age group SWB 0 since it is embedded in a young population environment (Chu & Kennicutt 1988).

From the locus of each object in Figures 2a and 2b, we obtained the SWB types, which are given in column (8) of Table 1. We also show in Table 1 the x - and y -coordinates in degrees (cols. [6] and [7]) with respect to the position of the cluster NGC 1928 ($\alpha_{1950} = 5^{\text{h}}21^{\text{m}}19^{\text{s}}$, $\delta_{1950} = -69^{\circ}31'30''$), which is located close to the geometrical center of the bar. Finally, the table notes contain additional information on particular objects (e.g., coordinates for new objects and subtracted superimposed stars).

4. SPATIAL DISTRIBUTION OF AGE GROUPS

We show in Figure 3a the spatial distribution of the whole sample. It consists of an approximately circular, densely populated central region (diameter $D \sim 6^{\circ}$) and a surrounding structure apparently separated by a gap from the central region; its southern part corresponds to the structure known as de Vaucouleurs' arm (Lyngå & Westerlund 1963). This ring becomes less defined in the western quadrant (toward the SMC and the

TABLE 3
PROPERTIES OF THE GROUPS

| Group (SWB) | Age (Myr) | Clusters ^a | Associations ^a | Total | M | m | M/m | PA | x_c | y_c |
|-------------|------------|-----------------------|---------------------------|-------|----------------------|----------------------|----------------------|-------------------|-----------------------|----------------------|
| 0 | 0–10 | 61 | 77 | 138 | 6.3 | 6.3 | 1.00 | 140° | -0°11 | 1°14 |
| I | 10–30 | 89 | 41 | 130 | 6.7 | 6.3 | 1.00 | 150 | -0.13 | 1.08 |
| II | 30–70 | 64 | 1 | 65 | 8.6 | 6.7 | 1.28 | 80 | 0.01 | 0.64 |
| III | 70–200 | 86 | 1 | 87 | 9.3 | 7.0 | 1.33 | 40 | -0.40 | 0.48 |
| IV A | 200–400 | 62 | 0 | 62 | 11.6 | 8.0 | 1.45 | 10 | -0.29 | 1.00 |
| IV B | 400–800 | 33 | 0 | 33 | 12.4 | 8.0 | 1.55 | 40 | -0.76 | -0.28 |
| V | 800–2000 | 41 | 0 | 41 | 13.3 | 10.5 | 1.27 | 40 | -0.66 | -0.55 |
| VI | 2000–5000 | 30 | 0 | 30 | 12.4 | 9.7 | 1.28 | 0 | -0.47 | -0.98 |
| VII | 5000–16000 | 38 | 0 | 38 | 17.0 | 10.7 | 1.59 | 40 | -0.86 | 1.34 |
| Total | 0–16000 | 504 | 120 | 624 | (25.5 ^b) | (15.6 ^b) | (1.63 ^b) | (0 ^b) | (-0.64 ^b) | (1.16 ^b) |
| | | | | | 25.5 ^b | 15.6 ^b | 15.6 ^b | 0 ^b | -0.28 | 0.68 |

^a Clusters include NC + C + CN + CA and associations NA + A + AN + AC.

^b Includes NGC 1841 and Reticulum.

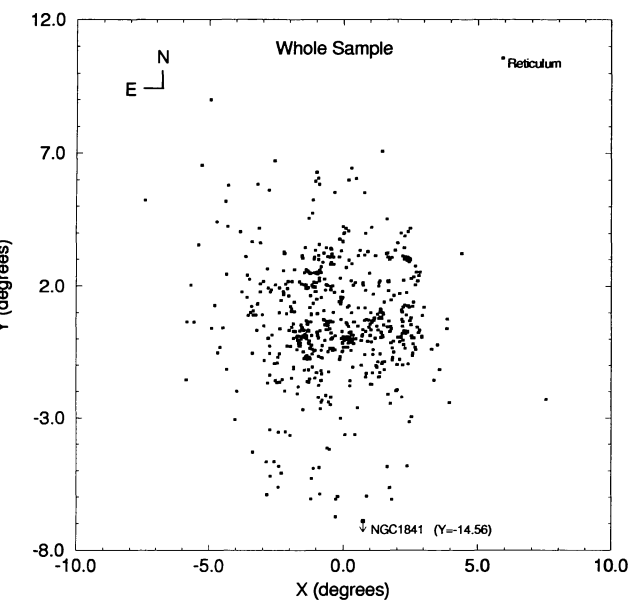


FIG. 3a

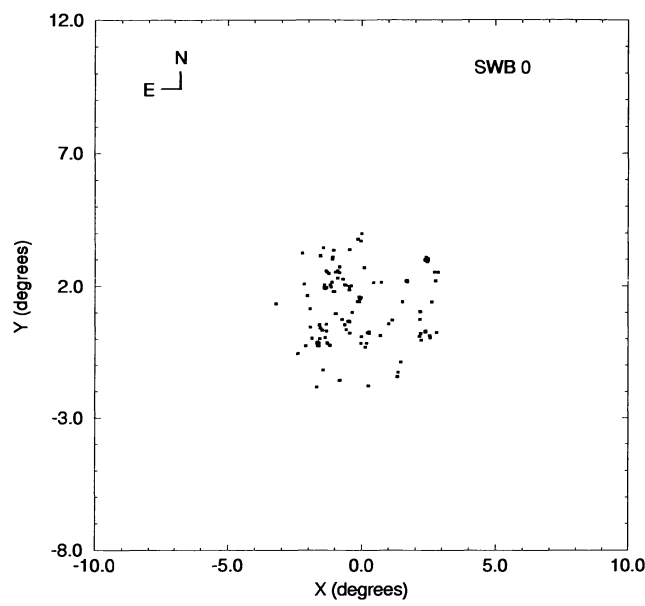


FIG. 3b

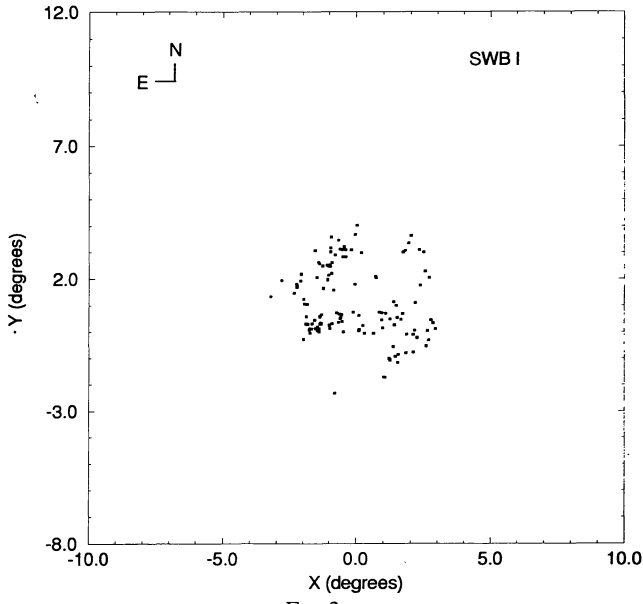


FIG. 3c

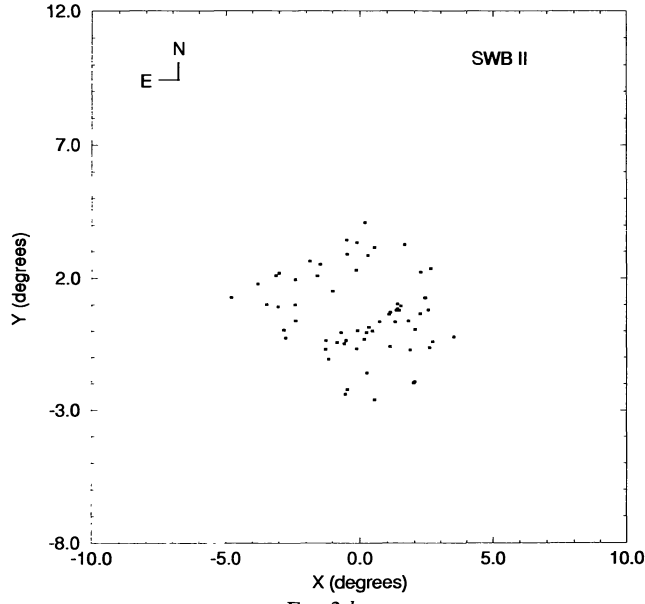


FIG. 3d

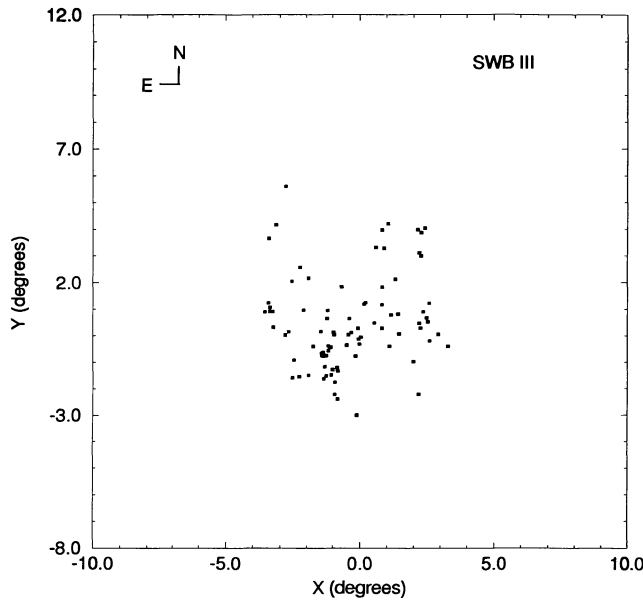


FIG. 3e

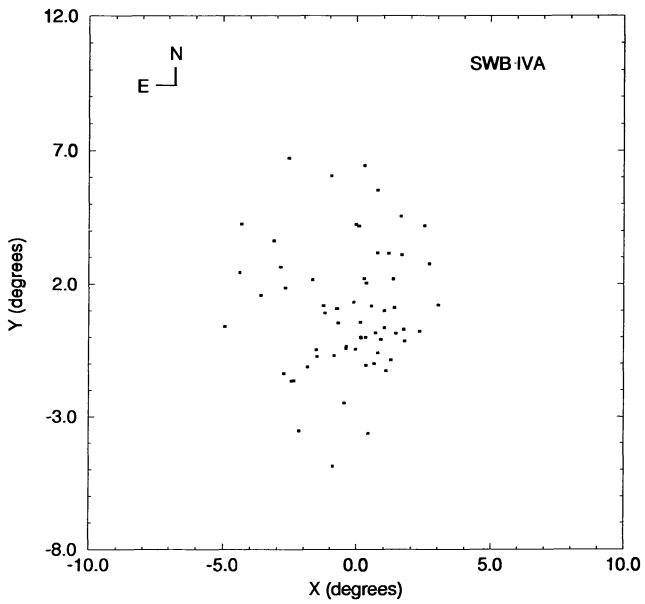


FIG. 3f

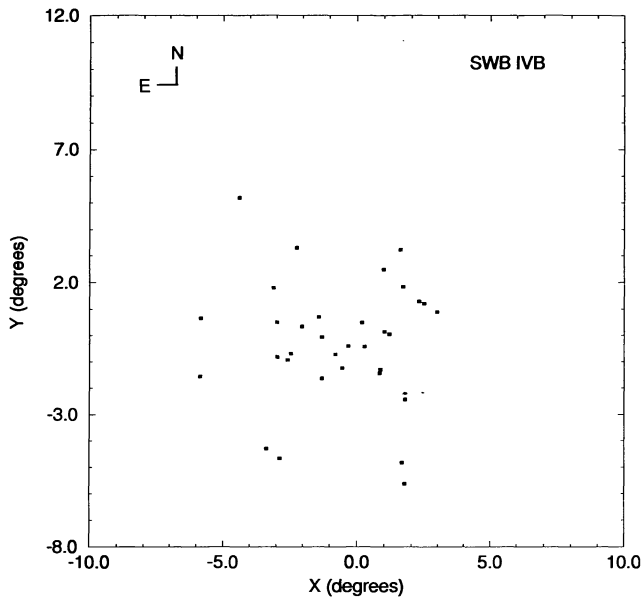


FIG. 3g

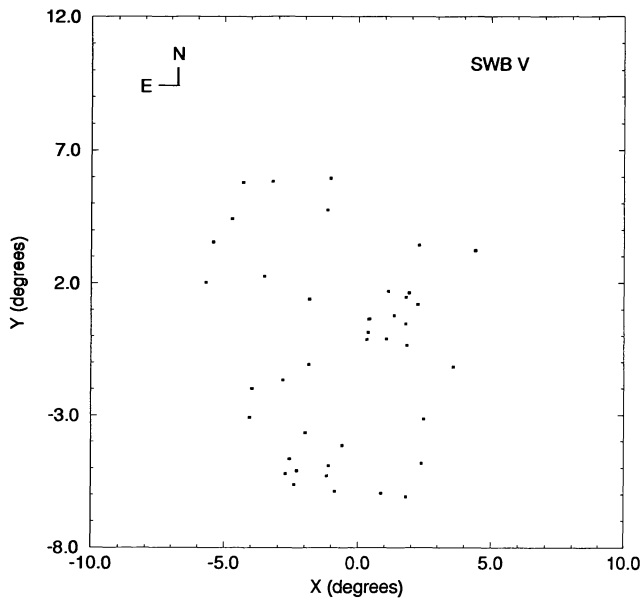


FIG. 3h

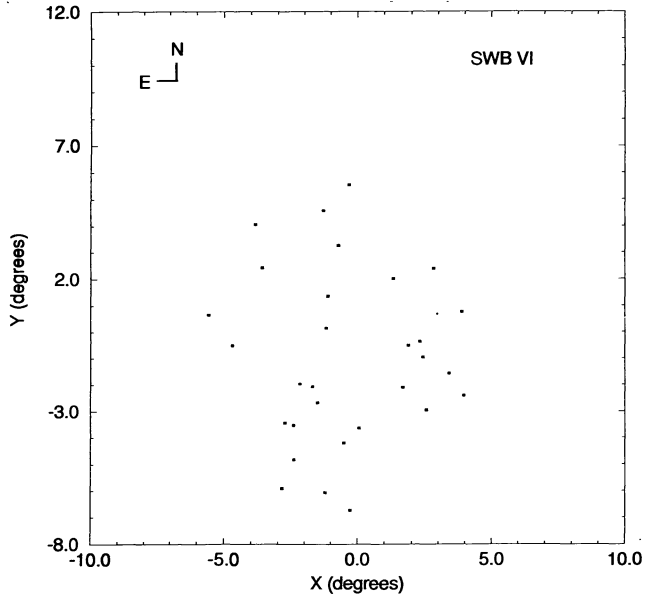


FIG. 3i

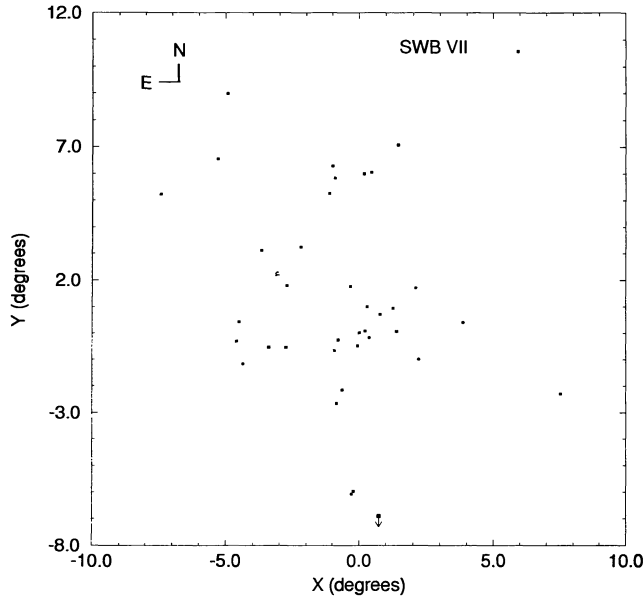


FIG. 3j

FIG. 3.—Spatial distributions: (a) whole sample, (b)–(j) age groups SWB 0 to SWB VII, respectively. NGC 1841 is outside the frame and is indicated by an arrow in (a) and (j).

Magellanic Stream), where clusters might have been stripped off, most likely because of the interaction between the LMC and SMC. The two outlying clusters are NGC 1841 (south) and Reticulum (northwest). The LMC bar can also be seen in Figure 3a.

The spatial distribution of the age groups from SWB 0 to SWB VII are shown in Figures 3b to 3j, respectively. A conspicuous property is the gradual shrinking of the spatial distribution toward the younger groups. We show in Table 3 the major (M) and minor (m) axes for each group together with the axial ratio (M/m) and the position angle (PA) of the major

axis (north = 0° , east = 90°). The oldest group (SWB VII) has a major axis ~ 3 times larger than that of the youngest group, SWB 0 (~ 4 times if NGC 1841 and Reticulum are included).

Interesting conclusions can be drawn on possible inclination changes of galaxy subsystems related to different age groups. The average axial ratio of the age groups from SWB II to SWB VII is 1.40 ± 0.14 (considering the inclusion or not of NGC 1841 and Reticulum), which suggests a tilt of $45^\circ \pm 4^\circ$ if the intrinsic distribution is assumed to be flat and circular. Under the same assumptions, the spatial distribution of the groups with ages in the range 0–30 Myr is nearly face-on.

The mean position angle of the major axis for the groups SWB III to SWB VII is $23^\circ \pm 15^\circ$. For the age group SWB II, it changes considerably ($PA = 80^\circ$), which suggests that its kinematic properties are intermediate between those of the very young, nearly face-on systems (SWB 0–I) and the older groups. Freeman, Illingworth, & Oemler (1983), studying radial velocities of 59 LMC clusters, reached similar conclusions, finding evidence of two disks with different kinematic properties. The differences in the kinematic behavior between the old and young age groups suggest that the LMC disk suffered a strong perturbation, possibly owing to an interaction with the SMC (see, e.g., Fujimoto & Murai 1984; Irwin 1991). Numerical simulations for the Cartwheel galaxy (Hernquist & Weil 1993), where the response of a self-gravitating disk galaxy with stars and gas to an axial collision with a less massive companion is studied, show that an outer ring is created (the LMC has a similar feature; see Fig. 3a) and the disk is heated and distorted, forming different subsystems in layers. It would be important to compute off-axis collisions to fit the LMC's properties, since the bar and the asymmetries in the disk evidenced in Figures 3a to 3j are not present in the Cartwheel galaxy. The spatial distribution of the group SWB 0 (Fig. 3b) presents some internal structure resembling arms, which is also present in Hernquist & Weil's (1993) simulations of the gas components (less pronounced in the stellar one), and in the Cartwheel galaxy as well. Group SWB I (Fig. 3c) has a bar structure that is rotated with respect to the LMC bar; a detailed discussion of this effect is given elsewhere (Dottori et al. 1995). Group SWB II (Fig. 3d) has a bar aligned to that of the galaxy, and the disk has an extension to the east. The intermediate-age group SWB V (Fig. 3e) has a clump of clusters at $x \sim 1.5^\circ$, $y \sim 1.0^\circ$, which corresponds to the western end of the bar. As shown in BCD92, there is an age gradient along the bar, younger to the east, which can also be observed by combining the present Figures 3e–3h (SWB III–V). Interestingly, in Hernquist & Weil's (1993) simulation, the stellar component reaches a quasi-stationary state in which a dense clump indicates the position where the companion crossed the disk; the spatial distributions of the groups SWB V and SWB IVA (Figs. 3f and 3g, respectively) present a comparable clump, located, however, off-center, which suggests a nonaxial impact of the SMC. In this scenario, the SWB IVA group would be part of a preexisting stellar disk, and its age (~ 300 Myr) would be an upper limit to the age of the collision. The large population of blue clusters in the LMC (Table 3) might have been the result of enhanced star formation during and after the collision. The enhanced star-formation epoch in the LMC at about 2 Gyr (see Mould 1992 and references therein) would have been originated in a previous event since the spatial distribution of the SWB V group ($0.8 \text{ Gyr} < \text{age} < 2.0 \text{ Gyr}$) presents a pattern characteristic of a perturbed stellar disk (Fig. 3h). In order to further test this scenario, numerical simulations should include the dynamical evolution of stars formed during and after the collision.

We calculated the centroid of each group (Table 3) and show their positions in Figure 4, where the error bars reflect the effect of suppressing points at the distribution edges. Also indicated are the geometric center of the bar (Bok 1966) and the center derived from the outer parts of the H I rotation curve (Rohlfs et al. 1984). The mean centroid of the blue groups (SWB 0 to SWB IVA) is located at $\sim 0.7^\circ$ (~ 0.7 kpc at the distance of the

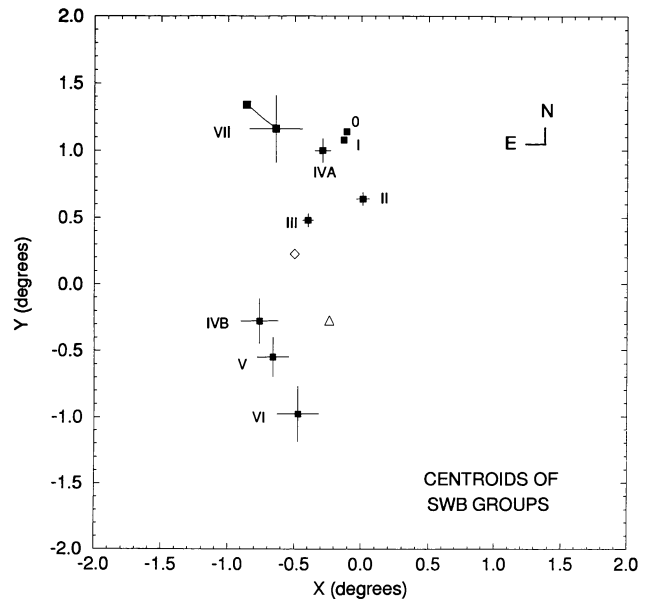


FIG. 4.—Centroids of the age groups are indicated by squares labeled with their respective SWB identifications. The diamond is the center of the H I rotation curve derived from the symmetry of its external parts (Rohlfs et al. 1984). The triangle is the geometrical center of the bar (Bok 1966). For SWB VII, the southwestern point includes the outlying clusters NGC 1841 and Reticulum, whereas the northeastern one excludes them.

LMC) to the northwest of the H I center. The centroids of the intermediate-age groups (SWB IVB to SWB VI) are located on the bar, at $\sim 0.6^\circ$ to the east of its geometric center. Finally, the old clusters (SWB VII) have a centroid $\sim 1.0^\circ$ north of the H I rotation-curve center. The noncoincidence of the centroids of the different age groups and that of the H I rotation curve certainly reflects the effects of a past perturbation suffered by the disks of stars and gas, which is also corroborated by the occurrence of structures such as off-center clumps, gaps, and the partial ring where, on the SMC, side clusters are missing.

5. CONCLUSION

A catalog of integrated *UBV* photometry of 504 star clusters and 120 stellar associations in the LMC, part of them still embedded in emitting gas, is provided in the present work, with $\sim 80\%$ of them collected by ourselves at CTIO and CASLEO. Age estimates in terms of the equivalent SWB classification were derived from the $(U - B) \times (B - V)$ diagram. The most excited H II regions are not located at the upper-left corner of the color-color diagram but around $(U - B) \sim -0.6$ mag and $(B - V) \sim -0.2$ mag, which is basically caused by the relative intensity of the emission lines and their distribution in the *UBV* filters. We provide a large sample of as yet unexplored SWB VII clusters in terms of H-R diagrams and RR Lyrae studies; follow-up works are necessary to check whether these clusters have ages of classical globular clusters or they occur in the apparent 3–10 Gyr age gap in the LMC. The oldest associations in the sample have embedded star clusters and are outlying objects in the young disk. The fraction of associations with emitting gas in the SWB 0 and SWB I types in the color-color diagram is significantly larger than that of star clusters

with emitting gas, which indicates that gas-sweeping mechanisms are more efficient in the clusters.

The size of the spatial distribution increases steadily with age (SWB type), whereas an axial-ratio difference exists between the groups respectively younger and older than 30 Myr, which suggests a nearly face-on orientation for the former and a tilt of $\sim 45^\circ$ for the latter groups. Asymmetries are present in the spatial distribution of the different age groups. The noncoincidence of the centroids of the different age groups and that of the H I rotation curve certainly reflects the effects of a past perturbation suffered by the disks of stars and gas. A comparison of the spatial distributions of the age groups and of the whole sample with the results of numerical simulations by Hernquist & Weil (1993) for the Cartwheel galaxy further suggests that a collision with the SMC has occurred. Simulations including

the dynamical evolution of stars formed during and after the collision are necessary in order to fit in detail the observed features in the LMC. Integrated *UBV* observations for a larger and fainter sample of clusters may reveal finer structures in the spatial distribution of the age groups, which in turn may set constraints on the age of the interaction between the Magellanic Clouds.

We thank the hospitality and assistance of the staffs at CTIO and CASLEO during the observations. We acknowledge support from the Brazilian institutions CNPq, FINEP, and FAPERGS and the Argentinian ones CONICET and CONICOR. We also acknowledge a grant from the Vitae Foundation. We thank Fábio Perosi for help with the tables and figures.

REFERENCES

- Alcaino, G., & Liller, W. 1982, *A&A*, 144, 213
 Arimoto, N., & Bica, E. 1989, *A&A*, 222, 89
 Bhatia, R. K., Read, M. A., Hatzidimitriou, D., & Tritton, S. 1991, *A&A*, 227, 335
 Bica, E., Alloin, D., & Santos, J. F. C., Jr. 1990, *A&A*, 235, 103
 Bica, E., Clariá, J. J., & Dottori, H. 1992, *AJ*, 103, 1859
 Bica, E., Clariá, J. J., Dottori, H., Santos, J. F. C., Jr., & Piatti, A. 1991, *ApJ*, 381, L51
 Bok, B. J. 1966, *ARA&A*, 4, 95
 Chiosi, C., Bertelli, G., & Bressan, A. 1988, *A&A*, 196, 84
 Chu, Y. H., & Kennicutt, R. C., Jr. 1988, *AJ*, 96, 1874
 Corsi, C. E., Buonanno, R., Fusi Pecci, F., Ferraro, F. R., Testa, V., & Greggio, L. 1994, *MNRAS*, 271, 385
 Davies, R. D., Elliot, K. H., & Meaburn, S. 1976, *MmRAS*, 81, 89
 Demers, S., & Kunkel, W. E. 1976, *ApJ*, 208, 932
 Dottori, H., & Bica, E. 1981, *A&A*, 102, 245
 Dottori, H., Bica, E., Clariá, J. J., & Puerari, I. 1995, *ApJ*, submitted
 Dufour, R. J., & Harlow, W. V. 1977, *PASP*, 89, 630
 Freeman, K. C., Illingworth, G., & Oemler, A., Jr. 1983, *ApJ*, 272, 488
 Fujimoto, M., & Murai, T. 1984, in *IAU Symp. 108, Structure and Evolution of the Magellanic Clouds*, ed. S. van den Bergh & K. S. de Boer (Dordrecht: Reidel), 115
 Girardi, L., & Bica, E. 1993, *A&A*, 274, 279
 Graham, J. A. 1982, *PASP*, 94, 244
 Gratton, R. G., & Ortolani, S. 1987, *A&AS*, 71, 131
 Henize, K. 1956, *ApJS*, 12, 163
 Hernquist, L., & Weil, M. L. 1993, *MNRAS*, 261, 804
 Heydari-Malayeri, M., Niemela, V. S., & Testor, G. 1987, *A&A*, 184, 300
 Hodge, P. W. 1960, *ApJ*, 131, 351
 —. 1988, *PASP*, 100, 1051
 Hodge, P. W., & Sexton, J. 1966, *AJ*, 71, 363
 Hodge, P. W., & Wright, F. W. 1967, *The Large Magellanic Cloud* (Smithsonian Pub. 4699) (Washington: Smithsonian Press)
- Irwin, M. J. 1991, in *IAU Symp. 148, The Magellanic Clouds and Their Interactions*, ed. R. F. Haynes & D. K. Milne (Dordrecht: Kluwer), 453
 Jensen, J., Mould, J., & Reid, N. 1988, *ApJS*, 67, 77
 Kontizas, E., Metaxa, M., & Kontizas, M. 1988, *AJ*, 96, 1625
 Kontizas, M., Morgan, D. H., Hatzidimitriou, D., & Kontizas, E. 1990, *A&AS*, 84, 527
 Lauberts, A. 1982, *The ESO/Uppsala Survey of the ESO (B) Atlas* (Munich: ESO)
 Lee, M. G. 1991, in *IAU Symp. 148, The Magellanic Clouds and Their Interactions*, ed. R. F. Haynes & D. K. Milne (Dordrecht: Kluwer), 207
 Lortet, M. C., & Testor, G. 1984, *A&A*, 139, 330
 Lucke, P. B., & Hodge, P. W. 1970, *AJ*, 75, 171
 Lyngå, G., & Westerlund, B. E. 1963, *MNRAS*, 127, 31
 Magalhães, A. M., Benedetti, E., & Roland, E. 1984, *PASP*, 96, 383
 Mateo, M., Hodge, P., & Schommer, R. A. 1986, *ApJ*, 311, 113
 Melnick, J. 1987, in *Observational Evidence of Activity in Galaxies*, ed. E. Ye. Khachikian, K. J. Fricke, & J. Melnick (Dordrecht: Reidel), 545
 Minitti, D., Clariá, J. J., & Gomez, M. N. 1989, *Ap&SS*, 158, 9
 Mould, J. R. 1992, in *IAU Symp. 149, The Stellar Populations of Galaxies*, ed. B. Barbuy & A. Renzini (Dordrecht: Kluwer), 181
 Mould, J. R., & Aaronson, M. 1980, *ApJ*, 240, 464
 Reed, B. C. 1985, *PASP*, 97, 120
 Robertson, J. W. 1974, *A&AS*, 15, 261
 Rohlfs, K., Kreitschmann, J., Siegman, B. C., & Feitzinger, J. V. 1984, *A&A*, 137, 343
 Santos, J. F. C., Jr., Bica, E., Clariá, J. J., Piatti, A., Girardi, L., & Dottori, H. 1995, *MNRAS*, in press
 Searle, L., Wilkinson, A., & Bagnuolo, W. 1980, *ApJ*, 239, 803
 Shapley, H., & Lindsay, E. M. 1963, *Irish Astron. J.*, 6, 74
 van den Bergh, S. 1981, *A&AS*, 46, 79
 —. 1991, *ApJ*, 369, 1
 Walker, A. R. 1991, in *IAU Symp. 148, The Magellanic Clouds and Their Interactions*, ed. R. F. Haynes & D. K. Milne (Dordrecht: Kluwer), 307